



รายงานวิจัยฉบับสมบูรณ์

โครงการ: การศึกษาเปรียบเทียบคุณสมบัติทางชีวเคมีและ  
ชีวฟิสิกส์ของเอนไซม์ที่ได้จากเหืองอกต่อมไทรอยด์  
ที่เป็นมะเร็งและไม่เป็นมะเร็ง

โดย: ดร.นิลุบล ปาริชาติธนกุล

พฤษภาคม 2556

รายงานวิจัยฉบับสมบูรณ์

โครงการ: การศึกษาเปรียบเทียบคุณสมบัติทางชีวเคมีและ  
ชีวฟิสิกส์ของเอนไซม์ที่ได้จากเหียงอกต่อมไทรอยด์  
ที่เป็นมะเร็งและไม่เป็นมะเร็ง

ผู้วิจัย: ดร.นิลุบล ปาริชาติธนกุล  
สังกัด: สถาบันวิจัยจุฬาภรณ์

สนับสนุนโดยสำนักงานกองทุนสนับสนุนการวิจัย  
และ สถาบันวิจัยจุฬาภรณ์ (ต้นสังกัด)

(ความเห็นในรายงานนี้เป็นของผู้วิจัย สกว.ไม่จำเป็นต้องเห็นด้วยเสมอไป)

## **Acknowledgments**

I would like to express my deepest appreciation to Prof. Emer. M.R. Jisnuson Svasti for his valuable advice and support. Moreover, I would like to thank Dr. Chantragan Srisomsap, Mr. Kittirat Saharat, Ms. Daranee Chokchaichamnankit and Ms. Pantipa Subhasitanont for contributing to this work. Special thanks to Prof. Johan R. Lillehaug from the University of Bergen, Norway, for graciously providing thyroid cancer cell lines and Assoc. Prof. Sr. Col. Phaibul Punyarit from Department of Pathology, Phramongkutklao College of Medicine, Thailand, for thyroid tissues (Institutional Review Board of the Royal Thai Army Medical Department S012H).

This research cannot be accomplished without the funding supported by the Thailand Research Fund for New Researchers and Chulabhorn Research Institute.

รูปแบบ **Abstract** (ภาษาอังกฤษ)

---

**Project Code :** TRG5380025

**Project Title :** Comparative biochemical and biophysical characterization of cathepsin B from benign and malignant thyroid tumors

**Investigator :** Dr. Nilubol Paricharttanakul, Chulabhorn Research Institute

**E-mail Address :** nilubol@cri.or.th

**Project Period :** 3 years (May 31, 2010 – May 30, 2013)

Proteomics have allowed for the identification of proteins as potential diagnostic or prognostic biomarkers of disease. In the case of thyroid cancer, which is the most common malignancy of the endocrine system, cathepsin B was shown to exhibit differential expression between normal and malignant tumors. In order to understand the relationship between protein expression and disease, the purification and characterization of cathepsin B isoforms from benign and malignant human thyroid tumors were proposed. Unfortunately due to limited tumor supply, two-dimensional immunoblots of cathepsin B isoforms were performed on papillary carcinoma (B-CPAP), follicular carcinoma (FTC-133) and anaplastic carcinoma (8305C) cell lines. This study revealed differential expression of different cathepsin B isoforms in the three cell lines, however expression was faint and detectable by immunoblotting. The isolation of cathepsin B isoforms would be challenging and this protein does not appear to have the characteristics of a good biomarker. However, proteomic analyses of B-CPAP and FTC-133 allowed for the identification and validation of five proteins with the potential to be used in a panel for diagnosis of well-differentiated thyroid cancers. The results from this research could have clinical application to improve the diagnosis of thyroid cancer with high accuracy and sensitivity.

**Keywords :** thyroid cancer, proteomics, biomarkers

## รูปแบบ บทคัดย่อ (ภาษาไทย)

รหัสโครงการ: TRG5380025

ชื่อโครงการ: การศึกษาเปรียบเทียบคุณสมบัติทางชีวเคมีและชีวฟิสิกส์ของเอนไซม์ที่ได้จากเนื้ออกต่อมไทรอยด์ที่เป็นมะเร็งและไม่เป็นมะเร็ง

ชื่อนักวิจัย: ดร.นิลุบล ปาริชาติธนกุล สถาบันวิจัยจุฬาภรณ์

E-mail Address : nilubol@cri.or.th

ระยะเวลาโครงการ: 3 ปี (31 พฤษภาคม 2553 ถึง 30 พฤษภาคม 2556)

โปรตีนโอมิกส์ เป็นวิธีการวิเคราะห์โปรตีนที่มีศักยภาพ ซึ่งสามารถใช้ค้นหาตัวบ่งชี้ทางชีวภาพเพื่อการวินิจฉัยและการทำนายการเกิดโรคได้ cathepsin B เป็นโปรตีนที่พบว่ามีแสดงออกที่แตกต่างระหว่างมะเร็งไทรอยด์กับเนื้ออกไทรอยด์ธรรมดา ดังนั้น เพื่อที่เข้าใจความสัมพันธ์ระหว่างการแสดงออกของ cathepsin B และโรคมะเร็งไทรอยด์ ผู้วิจัยจึงได้เสนอทำการแยกและศึกษาคุณลักษณะของ cathepsin B isoforms จากเนื้ออกไทรอยด์ธรรมดาและมะเร็งไทรอยด์ ผู้วิจัยทำการวิเคราะห์ cathepsin B isoforms โดยใช้ two-dimensional immunoblots ในเซลล์มะเร็งไทรอยด์ชนิดต่างๆ ได้แก่ papillary carcinoma (B-CPAP), follicular carcinoma (FTC-133) และ anaplastic carcinoma (8305C) ผลการทดลองพบว่ามีแสดงออกของ cathepsin B isoforms ที่แตกต่างกันในสาม cell lines แต่ระดับการแสดงออกอยู่ในปริมาณที่ต่ำมาก ทำให้การแยก cathepsin B isoforms เป็นไปได้ลำบาก ซึ่งทำให้ไม่น่าเหมาะสมที่จะนำมาศึกษาคุณสมบัติของตัวบ่งชี้ทางชีวภาพที่ดี อย่างไรก็ตาม การวิเคราะห์ทางโปรตีนโอมิกส์ของเซลล์ B-CPAP และเซลล์ FTC-133 ทำให้สามารถจำแนกและยืนยันได้ว่ามีโปรตีนจำนวน 5 ชนิดที่มีศักยภาพในการตรวจโรคมะเร็งไทรอยด์ชนิด well-differentiated thyroid cancers ผลการทดลองจากงานวิจัยนี้สามารถนำมาประยุกต์ใช้ในการตรวจทางคลินิกเพื่อช่วยในการวินิจฉัยโรคมะเร็งไทรอยด์ได้ถูกต้องและแม่นยำมากยิ่งขึ้น

คำหลัก : มะเร็งต่อมไทรอยด์ โปรตีนโอมิกส์ ตัวบ่งชี้ทางชีวภาพ

**Output จากโครงการวิจัยที่ได้รับทุนจาก สกว.**

1. ผลงานตีพิมพ์ในวารสารวิชาการนานาชาติ (ระบุชื่อผู้แต่ง ชื่อเรื่อง ชื่อวารสาร ปี เล่มที่ เลขที่ และหน้า)  
Manuscript in preparation
2. Poster Presentations
  - a. Paricharttanakul, N. M., Srisomsap, C. and Svasti, J. Differential expression of cathepsin B isoforms in thyroid cancer cell lines. The 7<sup>th</sup> Princess Chulabhorn International Science Congress, Bangkok, Thailand, November 29-December 3, 2012
  - b. Paricharttanakul, N. M., Saharat, K., Chokchaichamnankit, D., Srisomsap, C., Svasti, J. Quest for Thyroid Cancer Biomarkers. ประชุมนักวิจัยรุ่นใหม่พบเมธีวิจัยอาวุโส สกว. ครั้งที่ 12, Petchburi, Thailand, October 10-12, 2012
  - c. Distinguishing post-translational modifications in isoforms of cathepsin B from thyroid tumors. Paricharttanakul, N. M., Punyarit, P., Srisomsap, C. and Svasti, J.. The 3rd Biochemistry and Molecular Biology Conference, Chiangmai, Thailand, April 6-8, 2011
  - d. Comparative studies of cathepsin B as a biomarker for thyroid malignancy. Paricharttanakul, N. M., Subhasitanont, P., Punyarit, P., Srisomsap and Jisnuson Svasti. HUPO 9th Annual World Congress, Sydney, Australia, September 19–23, 2010

## Table of contents

Chapter	Section	Heading	Page
1		Proposal	
	1.1	Rationale and significance of research	1
	1.2	Objectives	3
	1.3	Materials and Methods	4
	1.4	Proposed timeline	7
	1.5	Proposed journal for publication	7
2		Characterization of cathepsin B from lysates of follicular adenoma and papillary carcinoma tissues	
	2.1	Introduction	8
	2.2	Enzymatic activity of cathepsin B	9
	2.3	Two-dimensional SDS-PAGE (2-DE)	11
	2.4	Two-dimensional immunoblotting	12
	2.5	Post-translational modifications	13
	2.6	Conclusion	15
3		Screening for thyroid cancer cell lines with the highest cathepsin B expression	
	3.1	Introduction	16
	3.2	Cell culture	16
	3.3	One-dimensional SDS-PAGE (1-DE)	17
	3.4	One-dimensional immunoblotting	18
	3.5	Two-dimensional SDS-PAGE (2-DE)	19
	3.6	Two-dimensional immunoblotting	23
	3.7	Conclusion	23
4		Identification of potential biomarkers for distinguishing between the well-differentiated thyroid cancers	
	4.1	Introduction	26
	4.2	Cell Culture	26
	4.3	Cytotoxicity of doxorubicin to BCPAP and FTC133 cell lines	27
	4.4	2-D PAGE and image analysis	28
	4.5	In-gel digestion and protein identification	28
	4.6	Western blot analyses	49
	4.7	Conclusion	55
5		Concluding remarks	56
6		References	58

## **Chapter 1. Proposal**

### **1.1. Rationale and significance of research**

Thyroid cancer is the most common malignancy of the endocrine system, though relatively uncommon among all cancers. Risk factors include being of Asian race, female gender, family histories of thyroid diseases and radiation exposure of the head and neck (1). 37,200 new cases of thyroid cancer with 1,630 deaths were estimated by the National Cancer Institute to be diagnosed in the United States in 2009. Thyroid cancer incidence rates for Asians are 4.2 and 14.2 per 100,000 men and women, respectively, with mortality rates of 0.4 and 0.7 per 100,000 men and women, respectively (2). According to the Thai National Cancer Institute Registry, thyroid cancer cases were reported in 2006 to be 0.7% and 1.5% of all cancer cases reported in men and women, respectively (3).

There are four types of thyroid cancer; the most common occurring in 70-80% of cases is papillary carcinoma, followed by follicular carcinoma (10-15%), medullary carcinoma (5-10%) and anaplastic carcinoma occurring in less than 5% of all cases (4). Prognosis is best for papillary carcinoma, especially in young patients whose nodules are confined to the thyroid gland. Thyroid cancer is generally diagnosed by biopsy of the thyroid nodule, and evaluated by determining the levels of thyroxine (T4), thyroid stimulating hormone (TSH) and a thyroid cancer marker, thyroglobulin, in the blood and/or a whole body iodine scan. However, antibodies in the blood can interfere with thyroglobulin levels, resulting in inaccuracy in measurements (4). Therefore, new markers for thyroid cancer are necessary for accurate diagnosis and prognosis.

Cathepsin B, a cysteine protease implicated in tumor invasion and metastasis, has been identified to be a potential biomarker for neoplastic thyroid diseases (5). Proteomic studies on human thyroid tissues distinctly pinpointed cathepsin B to be significantly expressed with differing protein patterns in the nonmalignant neoplastic disease, follicular adenoma, and the malignant follicular carcinoma and papillary carcinoma, as shown in Figure 1.1. Understanding the distinct characteristics of the protein from the nonmalignant and the malignant thyroid diseases could provide insight into differential diagnosis using cathepsin B as a malignant biomarker.



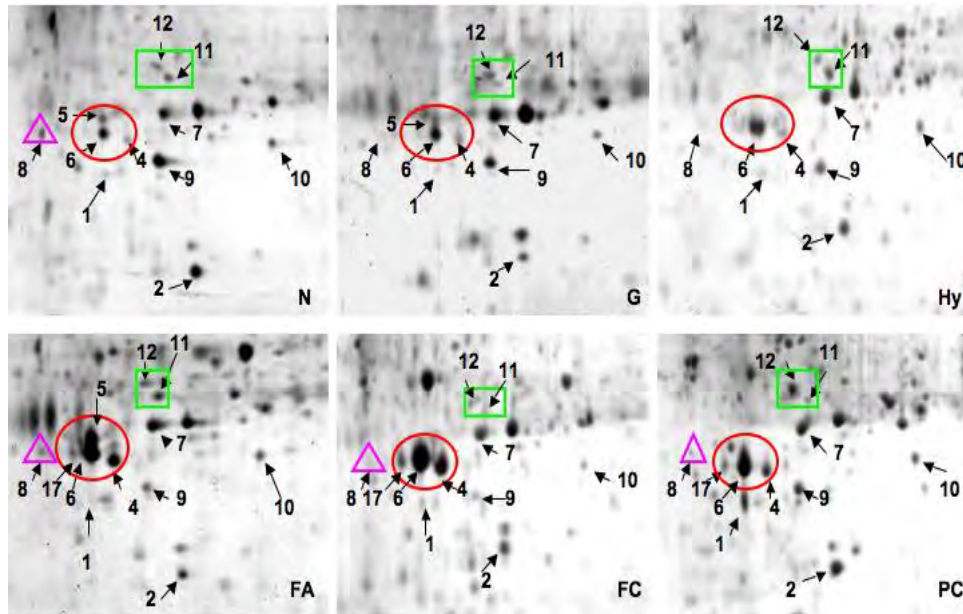


Figure 1.1. Two-dimensional PAGE of thyroid tissues. Normal (N), multinodular goiter (G), diffuse hyperplasia (Hy), follicular adenoma (FA), follicular carcinoma (FC) and papillary carcinoma (PA) were compared. The spots circled in red were identified by mass spectrometry to be cathepsin B. Picture courtesy of Srisomsap C. (5).

Cathepsin B is a lysosomal protease important for intracellular proteolysis and is distributed in various tissues in the body, including liver, kidney and spleen (6). This protease belongs to the cysteine protease family in the papain superfamily. It is synthesized as an inactive proenzyme that becomes targeted to the lysosome for processing into the active enzyme form (7). Cathepsin B is involved in the post-translational processing of active proteins from their inactive precursors, e.g., insulin from proinsulin in the pancreas and albumin from proalbumin in the liver (8). Moreover, cathepsin B is capable of degrading extracellular matrix proteins directly by proteolysis or indirectly by activating other extracellular matrix proteases (7). This capability allows for the detachment of tumor cells from the extracellular matrix and thus implicated cathepsin B in tumor malignancy and metastasis (9). The activity of cathepsin B was recently reported to be increased in breast cancer, prostate cancer and early stage gastric carcinoma, and be correlated to the degree of invasiveness of the cancers (9).

Cathepsin B is a bifunctional enzyme with endopeptidase and dipeptidyl carboxypeptidase activities. After limited proteolysis, the active enzyme contains two chains, a light chain (~5kDa) and a heavy chain (~25kDa), linked by a disulfide bridge (10). The

enzyme contains six disulfide bonds with two unpaired cysteines, one of which is a reactive cysteine (Cys29). The crystal structure of the human liver cathepsin B revealed the importance of two histidine residues, His110 and His111, in the large insertion loop or “occluding loop” in conferring the dipeptidyl carboxypeptidase activity (11). Site-directed mutagenesis of the interactions holding the insertion loop enhanced the endopeptidase activity of cathepsin B, possibly due to the increased flexibility of the loop. Changes in the positioning of this loop could be important for promoting protein-protein interactions in pathological conditions, e.g., tumor invasion and metastasis, and have become targets for inhibitor design (12).

Cathepsin B is a glycoprotein, whose isoforms have been detected and isolated from porcine liver (13), porcine spleen (14), bovine liver (15) and human hepatoma HepG2 cells (16). Moreover, cathepsin B may or may not exist in multiple isoforms depending on the species or tissues (6). However, the carbohydrate moiety of cathepsin B has been reported not to influence enzymatic activity *in vitro* (12, 16). It is noteworthy to report that in human thyroid tissues, not only are the levels of cathepsin B greatly elevated in thyroid diseases when compared to normal tissues, but also isoforms of cathepsin B exist and are different between malignant and non-malignant tissues (5).

In human thyroid, the function of cathepsin B is two-fold. Not only does cathepsin B acts to cleave thyroglobulin, thus releasing hormones into the circulatory system, it also functions in protein degradation (17). This proteolytic activity has been suggested to correlate with the invasiveness of the cancer. Therefore, the goal of this study is to purify and isolate the different isoforms of cathepsin B from benign and malignant tumors to compare their characteristics and investigate their ability to induce invasion of cancer cells. The differences in cathepsin B isoforms from the two sources could provide key information for understanding the correlation with malignancy in thyroid cancer.

## **1.2. Objectives**

The objective of this study is to understand the role of cathepsin B in thyroid cancer, with the following specific aims:

1. To purify cathepsin B from malignant and benign thyroid tumors
2. To isolate isoforms of cathepsin B from malignant and benign tumors

3. To characterize the folding and stability of purified cathepsin B from malignant and benign tumors, and their isoforms
4. To investigate the differences in post-translational modifications in the cathepsin B isoforms
5. To ascertain whether isoforms of cathepsin B from malignant and benign tumors induce differential invasiveness of cancer cells

## **2.3. Materials and Methods**

### **Tissues**

Human thyroid tissues confirmed by histology to be follicular adenoma (FA), and papillary carcinoma (PC) will be provided frozen by the Pathology Department, Phramongkhutkiao Hospital. HepG2 cells will be cultured in DMEM containing 10% fetal bovine serum, 100 U/ml penicillin, 100 µg/ml Streptomycin and 125 ng/ml amphotericin B at 37°C in a humidified atmosphere of 5% CO<sub>2</sub>.

### **Extraction and purification of cathepsin B**

The extraction and purification protocols from the FA and PC tissues will follow that of the purification of porcine parathyroid cathepsin B (8). Tissues will be thawed and homogenized. After centrifugation, the supernatant will be subjected to acetone precipitation. The pellets will be assayed for cathepsin B activity and the active pellet purified. Purification protocols to yield active cathepsin B using ion-exchange and gel filtration chromatography will be attempted.

### **Separation of the different isoforms**

Purified protein will be subjected to concavalin A-Sepharose 4B and eluted with methyl- $\alpha$ -D-glucopyranoside. This should separate the isoforms based on the carbohydrate binding ability. However if unsuccessful, then the purified protein will be loaded on gel filtration or ion-exchange columns to separate the different isoforms for further studies (15).

### **Cathepsin B activity assays**

The hydrolysis of Z-Arg-Arg-NHMec (NHMec is 7-amino-4-methylcoumarin) by cathepsin B will be measured fluorometrically (18). The enzyme will be activated with 5 mM DTT and 2.5 mM EDTA, pH 5.2 for 10 minutes at 37°C. 5 mM of the substrate, Z-Arg-Arg-NHMec in 0.1 M sodium phosphate buffer, pH 6.2, will be added to start the reaction. After incubating for 15 minutes, the reaction will be stopped with monochloroacetate, pH 4.3, and the release of NHMec measured using a fluorimeter at an excitation wavelength of 370 nm and an emission wavelength of 460 nm. One unit of enzyme activity is defined as the amount of enzyme required for the release of 1 micromole NHMec/minute.

### **Protein determination**

Protein concentration will be determined using the Bio-Rad Protein Assay, following the instructions provided by the manufacturer.

### **Polyacrylamide gel electrophoresis**

For one-dimensional gel electrophoresis, 12.5% Tris-glycine polyacrylamide gels will be used in the presence of SDS in the buffer system described by Laemmli using a Hoefer system and stained by Coomassie Brilliant Blue. For two-dimensional gel electrophoresis, proteins will be incubated in lysis for two hours at room temperature and applied by overnight in-gel rehydration of nonlinear pH 3-10 immobilized strips. Isoelectric focusing will be performed, and strips will be equilibrated in equilibration buffer containing DTT for 10 minutes at room temperature, and another 10 minutes in equilibration buffer with iodoacetamide instead of DTT. The IPG strips will be applied on 12% SDS-PAGE, and electrophoresis performed (19). Proteins on the gel will then be stained with Coomassie Brilliant Blue or SYPRO ruby for detection.

### **Immunoblotting for validation**

After electrophoresis is performed, the separated proteins will be transferred to a nitrocellulose membrane using the Bio-Rad Mini Trans-Blot cell at 100V for 30 minutes at

4°C (18). The membrane will be blocked with 5% non-fat dried milk for one hour at room temperature, and probed with mouse anti-cathepsin B monoclonal antibody in 20 mM Tris-buffered saline pH 7.6 with 0.1% Tween 20, overnight at 4°C. The membrane will be repeatedly washed in the same buffer and incubated in 1:5000 horseradish peroxidase-conjugated anti-mouse IgG for one hour. The reaction will be developed using the enhanced chemiluminescence (ECL) plus detection system, with high performance film.

### **Post-translational modification analysis**

To detect the type of post-translational modification present in the different isoforms of cathepsin B, SDS-PAGE will be performed and stained using pro-Q diamond phosphoprotein gel stain or pro-Q emerald glycoprotein gel stain, following the instructions provided by Invitrogen.

### **Carbohydrate analysis**

Purified protein will be denatured with SDS and 2-mercaptoethanol, incubated with PNGase F at 37°C for 18 hours or endoglycosidase F at 37°C for 1 hour, and subjected to SDS-PAGE and HPLC for analysis.



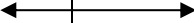


### **Circular Dichroism Measurements**

Measurements for cathepsin B from the two sources will be compared on a Jasco spectropolarimeter (20). Wavelength scans on 0.1 mg/ml protein will be measured at 25°C in peltier temperature controlled holders from 190-260nm at 20nm/min with 8 seconds response time. Thermal unfolding of the protein will be monitored at the wavelength giving the maximal ellipticity (~215-220 nm) from 0 to 100°C with a 0.2°C step size at 1°C/min heating rate and 16 seconds response time. After complete unfolding, the samples will be cooled to 25°C for a final wavelength measurement scan. The fraction unfolded will be calculated by normalizing the thermal unfolding profiles.

## Invasion assay

The ability of the isoforms of cathepsin B from benign and malignant tumors to facilitate HepG2 cells to invade Matrigel Basement Membrane Matrix will be assayed.  $1 \times 10^5$  cells (200 ml) HepG2 cell suspension will be seeded onto the upper Transwell cell culture chamber with filter coated with 30 mg Matrigel, in the absence as control and presence of each isoform of cathepsin B. Hepatocyte growth factor will be added in the lower chamber as chemoattractant. Cells that invade will go through the filter and attach to the undersurface of the upper chamber. Cells on the upper surface will be removed by swabbing using a cotton swab, and the filter fixed with 25% methanol and stained with 0.5% (w/v) crystal violet solution (21). The number of invaded cells in the presence of cathepsin B will be counted under a microscope and compared to that in the absence of cathepsin B.

## 2.4. Proposed timeline

	Year 1		Year 2	
	1 <sup>st</sup> half	2 <sup>nd</sup> half	1 <sup>st</sup> half	2 <sup>nd</sup> half
1. Optimize the purification of cathepsin B from benign and malignant tumors				
2. Optimize isoform isolation				
3. Identify the type of post-translational modification in cathepsin B by -Phosphoprotein staining -Glycoprotein staining -Deglycosylation				
4. Characterize cathepsin B -folding and stability -invasion ability				
5. Prepare manuscript				

## 2.5 Proposed journal for publication

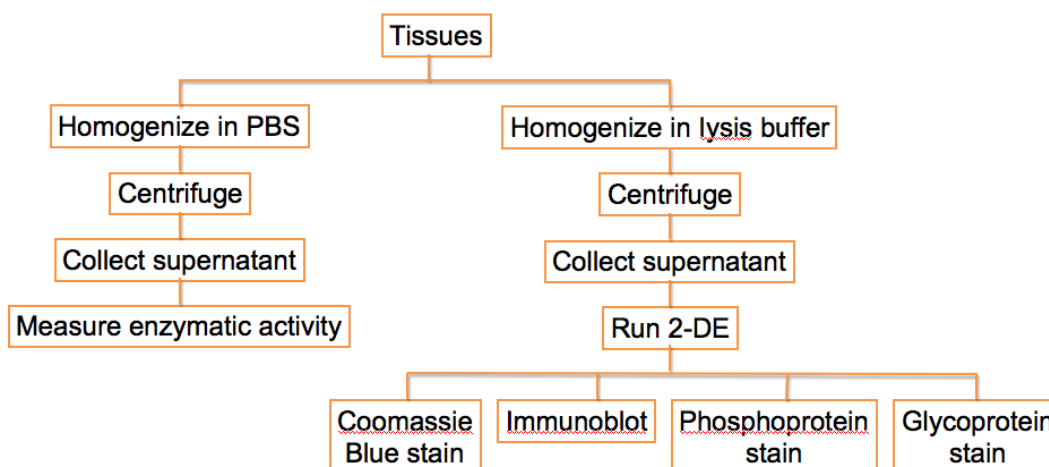
Cell Biology and Biophysics or Journal of Biochemistry

## Chapter 2. Characterization of cathepsin B from lysates of follicular adenoma and papillary carcinoma tissues

### 2.1 Introduction

Cathepsin B, a cysteine protease implicated in tumor invasion and metastasis, has been identified to be a potential biomarker for neoplastic thyroid diseases. In human thyroid tissues, not only are the levels of cathepsin B greatly elevated in thyroid diseases when compared to normal tissues, but also isoforms of cathepsin B exist and are different between malignant and non-malignant tissues. Understanding the distinct characteristics of the protein from the nonmalignant and the malignant thyroid diseases could provide insight into differential diagnosis using cathepsin B as a malignant biomarker.

In this study, we compared a benign thyroid tumor classified as follicular adenoma with a malignant thyroid tumor type of papillary carcinoma using enzymatic assays, two-dimensional polyacrylamide gel electrophoresis, immunoblotting and specific stains. Proteomic studies, comparing a nonmalignant (follicular adenoma) and a malignant (papillary carcinoma) thyroid tissue, allow for the identification of cathepsin B as a potential biomarker for thyroid neoplasm. Herein, we followed the following strategy to further characterize and compare cathepsin B from both tissues.



Approximately 20 mg of each tissue was manually homogenized in either phosphate buffer saline for activity assays or lysis buffer (7 M urea, 2 M thiourea, 4% CHAPS, 2% DTT, 2% Ampholine pH 3-10) for gel electrophoresis and immunoblots. After an hour of incubation on ice and a 10-minute centrifugation at 12,000 rpm, the supernatants were collected and protein concentration determined by Biorad protein assay using immunoglobulin G as standard.

## **2.2. Enzymatic activity of cathepsin B**

Appropriate dilutions of enzyme were prepared in 0.1% Brij. After pre-incubation of 50  $\mu$ l diluted enzyme in 25  $\mu$ l stock buffer (100mM sodium phosphate buffer pH 6.0, 2.5mM EDTA, 5mM DTT) for 15 minutes at 37°C, the reaction was started with 25  $\mu$ l freshly diluted 0.02 mM Z-Arg-Arg-NHMec (final concentration of 5  $\mu$ M) and incubated for 10 minutes at 37°C. The reaction was stopped with 100  $\mu$ l 100mM sodium monochloroacetate, pH 4.3 and measured using a fluorescence plate reader with excitation and emission wavelengths of 370 nm and 460 nm, respectively. For inhibition studies, after 10 minutes of pre-incubation of diluted enzyme in stock buffer, 1  $\mu$ l of 10 mM CA-074 (final concentration 0.1 mM) was added and incubated for five minutes at 37°C before starting the reaction.

The ability to cleave substrate, Z-Arg-Arg-NHMec, as shown by the increase in fluorescence intensity, of cathepsin B in papillary carcinoma was higher than that of follicular adenoma by 1.3-fold at saturating concentrations of substrate (Figure 2.1 top panel). Moreover, at non-saturating concentrations of substrate, linearity was observed in both cases with slopes of 173.8 and 15.7 for papillary carcinoma and follicular adenoma, respectively. Thus, the ability to cleave substrate by cathepsin B was greater for papillary carcinoma than follicular adenoma by eleven-fold as shown in the bottom panel of Figure 2.1.

To ensure that the enzymatic activities measured were specific to cathepsin B and not to other cathepsins, a selective inhibitor CA-074 [N-(L-3-trans-propylcarbamyloxirane-2-carbonyl)-L-isoleucyl-L-proline] was used to probe the biological function of cathepsin B. Figure 2.2 illustrates the effectiveness and specificity of CA-074 as an inhibitor of cathepsin B in both tissues as the activities of cathepsin B in the presence of inhibitor in both tissues were completely abolished to the same extent as blank.



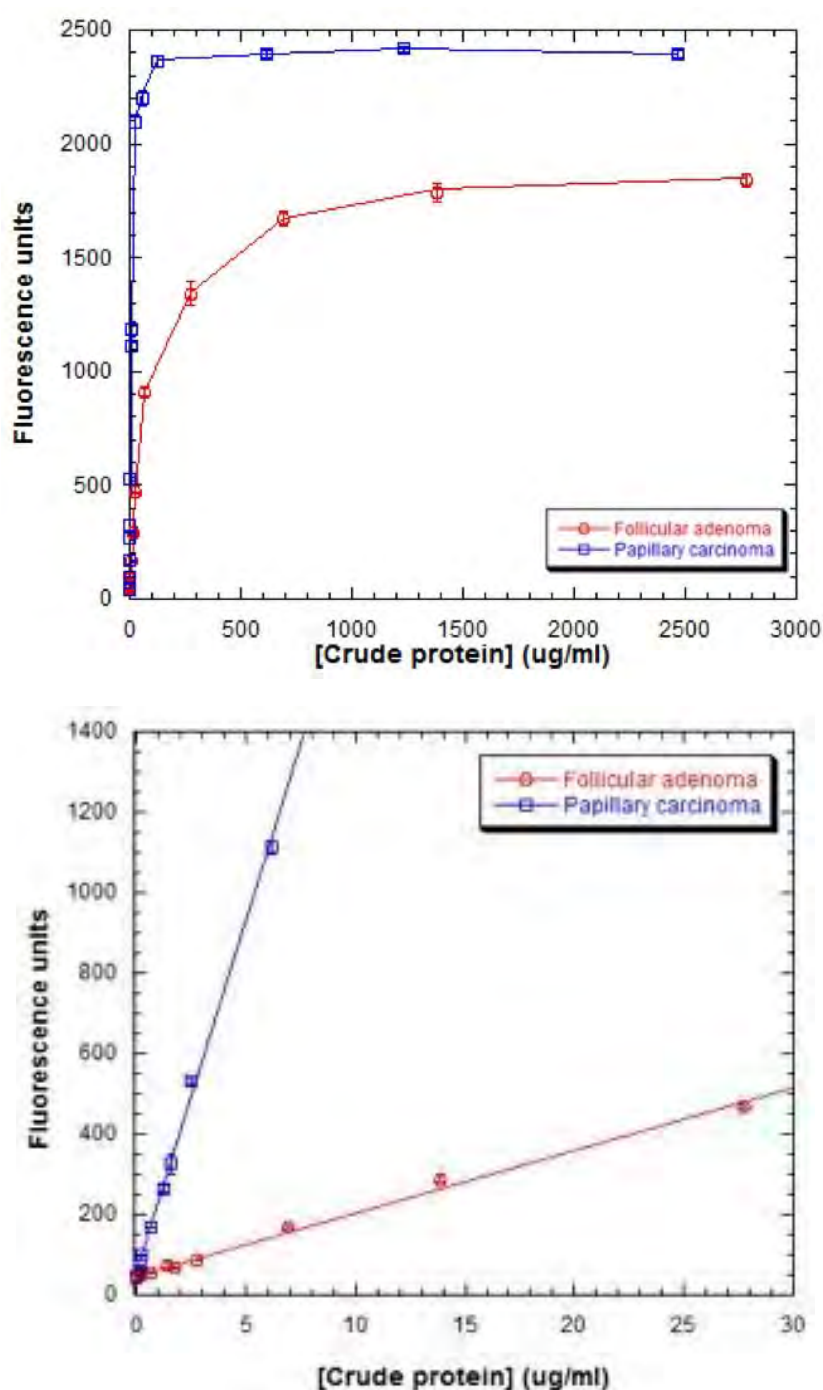


**Figure 2.1. Cathepsin B activities in lysates of follicular adenoma and papillary carcinoma tissues.** The top panel illustrates the enzymatic activities of cathepsin B using 5 mM Z-Arg-Arg-NHMeC as substrate. The bottom panel shows the linearity in activities at non-saturating concentrations revealed slopes of 15.7 and 173.8 for follicular adenoma and papillary carcinoma, respectively.

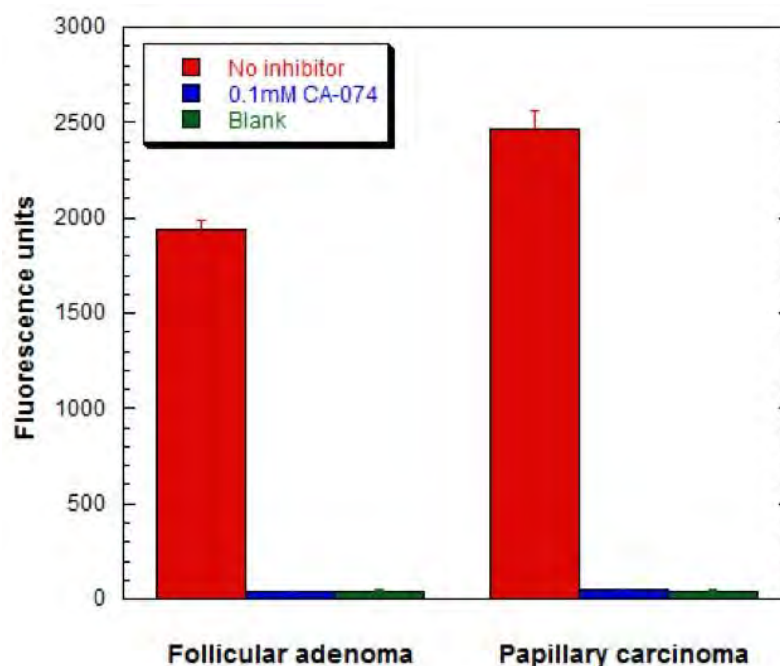


**Figure 2.2. Inhibition of cathepsin B activities by CA-074.** At 1:10 dilution of crude lysates corresponding to 1233  $\mu\text{g/ml}$  protein from papillary carcinoma and 1388  $\mu\text{g/ml}$  from follicular adenoma, cathepsin B activities were compared at 5  $\mu\text{M}$  substrate in the absence and presence of 0.1 mM CA-074. Blank does not contain lysates.

### 2.3. Two-dimensional SDS-PAGE

Two-dimensional polyacrylamide gel electrophoresis (2-DE) is a powerful tool to study proteins separated by their isoelectric points and molecular weights. It allows for the visualization of total protein content and their isoforms in crude lysates. Samples were applied by overnight in-gel rehydration on 7 cm, nonlinear pH 3–10 IPG gel strips and run on IPGphor at 7000 Vh. Focused IPG strips were equilibrated for 10 minutes in a solution (6 M urea, 30% glycerol, 1% SDS, 1% DTT in 50 mM Tris-HCl buffer, pH 6.8), and then for an additional 10 minutes in the same solution except that DTT was replaced by 2.5% iodoacetamide. The IPG strips were then applied on 12.5% SDS-PAGE in a Hoefer system at 10 mA for 3 hours at room temperature. Gels were then stained with 0.1% Coomassie Blue overnight, destained with 40% methanol, 10% acetic acid, and then scanned. One isoform and three isoforms of cathepsin B were detected in follicular adenoma and papillary carcinoma, respectively, as shown in Figure 2.3.

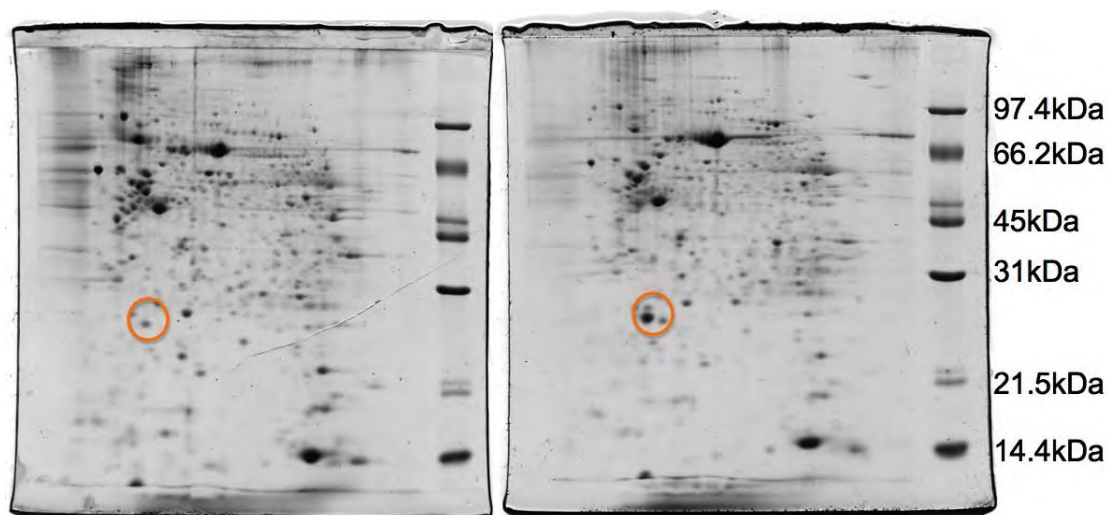


**Figure 2.3. Two-dimensional SDS gel electrophoresis of follicular adenoma (A) and papillary carcinoma (B) tissues.** Cathepsin B isoforms, as confirmed by N-terminal sequencing and LC/MS/MS, are circled.

#### 2.4. Two-dimensional immunoblotting

In order to confirm that the spots circled in 2-DE gels were indeed cathepsin B isoforms, immunoblotting was performed using cathepsin B antibody. After electrophoresis, proteins were transferred to nitrocellulose membranes at 100 V for 1.5 hours at 4 °C. After blocking in 5% non-fat dry milk, membranes were probed with 1:400 diluted cathepsin B monoclonal antibody for 1 hour, repeatedly washed in 20 mM Tris buffered-saline, pH 7.6, containing 0.1% Tween 20, and then incubated in 1:5000 horseradish peroxidase-conjugated rabbit anti-mouse immunoglobulin for 1 hour. After repeated washing, the reaction was developed using the enhanced chemiluminescence (ECL) plus detection system, with high performance film.

2D immunoblots of lysates of follicular adenoma and papillary carcinoma revealed three isoforms of cathepsin B in both follicular adenoma and papillary carcinoma, with differential expression as shown in Figure 2.4. Cathepsin B isoforms were detected with higher sensitivities using Western blots as compared to Coomassie stain. Coomassie stain was only able to detect one isoform and three isoforms of cathepsin B in follicular adenoma and papillary carcinoma, respectively. Immunoblotting using cathepsin B antibody was able to detect two more isoforms in follicular adenoma, with much lower expression levels.

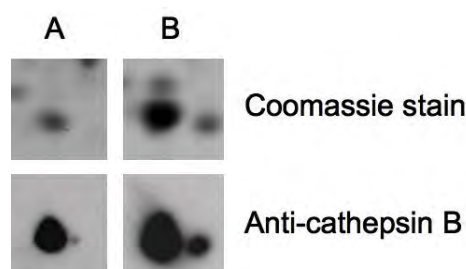


**Figure 2.4. Detection of cathepsin B isoforms in 2D immunoblots of follicular adenoma (A) and papillary carcinoma (B) tissues.** Three isoforms of cathepsin B were detected in 2D Western blots using monoclonal cathepsin B antibody, with differential expression.

For immunoblotting of O-GlcNac proteins, after electrophoresis, proteins were transferred to polyvinylidene difluoride membranes at 100 V for 1.5 hours. The membranes were then soaked in 100% methanol for two minutes, dried and probed with 1:5000 diluted O-GlcNac antibody (CTD110.6) in 1% casein blocking buffer overnight at 4°C. After extensive washing, the membranes were incubated with horse horseradish peroxidase-conjugated goat anti-mouse immunoglobulin M for 1 hour. After repeated washing, the reaction was developed using the enhanced chemiluminescence (ECL) plus detection system, with high performance film. After developing, the membranes were stained in 0.1% Coomassie Blue for 1 minute before destaining in 40% methanol, 10% acetic acid to compare with film. The results are discussed in the next section.

## 2.5. Post-translational modifications

As most proteins undergo some form of post-translational modifications, we want to investigate whether these modifications may be associated with disease states, in our case, benign and malignant thyroid tumors. Phosphorylation on serine, threonine or tyrosine residue is one of the most common post-translational modifications found in living organisms as it is involved in signal transduction and thus regulation of biological activities of proteins. Glycosylation is another post-translational modification with significant effects on protein folding, conformation, stability and activity. Glycosylation involves the addition of sugar-moieties to proteins, ranging from simple monosaccharides to highly complex branched polysaccharides. There are two types of glycosylation: asparagine-linked (N-linked) or serine/threonine (O-linked) oligosaccharides which are major structural components of many cell surface and secreted proteins.

Phosphorylation and glycosylation of cathepsin B isoforms in follicular adenoma and papillary carcinoma tissues were evaluated using Pro-Q Diamond phosphoprotein and Pro-Q Emerald 488 glycoprotein gel stains, respectively.

Pro-Q Diamond phosphoprotein gel stain is a fluorescent gel stain from Invitrogen, with excitation/emission maxima of approximately 555/580 nm, and detects the phosphorylation status of proteins. This stain is sensitive for detection of nanogram levels of protein. Using this stain on 2-DE gels loaded with 300 µg total protein, phosphorylation of cathepsin B isoforms was detected in papillary carcinoma but not in follicular adenoma as shown in Figure 2.5 following manufacturer's instructions.

Detection of glycosylated proteins in gels can be accomplished by using Pro-Q Emerald 488 glycoprotein gel stain by Invitrogen. This stain reacts with periodate oxidized carbohydrate groups with excitation/emission maxima of 510/520 nm, emitting a bright green fluorescent signal on glycoproteins. Depending on the degree and nature of glycosylation, this stain can detect as little as 4 ng of glycoprotein. Using this stain on 2-DE gels loaded with 150 µg total protein, glycosylation of cathepsin B isoforms was detected in papillary carcinoma and faintly in follicular adenoma as shown in Figure 5 following instructions from the manufacturer.

The presence of a particular type of glycosylation, O-linked N-acetylglucosamine (O-GlcNac), was also studied using monoclonal antibody against O-GlcNac (CTD110.6) in the two tumors. CT110.6 recognizes specifically O-GlcNac in  $\beta$ -O-glycosidic linkage to both serine and threonine. O-GlcNac is important in transcription, proliferation and apoptosis, and thus proposed to be prevalent in cancer. O-GlcNac modification is dynamic and has been suggested to have a reciprocal relationship with phosphorylation. As both phosphorylation and glycosylation were detected using the specific stains, the type of glycosylation in some isoforms of cathepsin B could be O-GlcNac. Two isoforms of cathepsin B with similar molecular weights were positive for O-GlcNac in papillary carcinoma, and only one in follicular adenoma at the same molecular weight as shown in Figure 5.

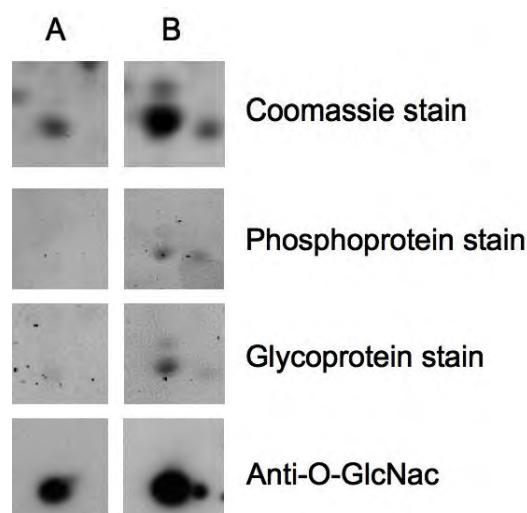


**Figure 2.5. Detection of post-translational modifications in cathepsin B isoforms in 2-DE gels and in 2D immunoblots of follicular adenoma (A) and papillary carcinoma (B) tissues.** Phosphorylation was detected in all three isoforms of cathepsin B only in papillary carcinoma using the Pro-Q Diamond phosphoprotein stain. Using the Pro-Q Emerald 488 glycoprotein stain, glycosylation of three isoforms of cathepsin B (1 major, 2 minor spots) was detected in papillary carcinoma, whereas only one isoform of cathepsin B was faintly detected in follicular adenoma. O-GlcNac immunoblots revealed two isoforms of cathepsin B with similar sizes in papillary carcinoma and one isoform in follicular adenoma.

## 2.6. Conclusion

The ability to cleave substrate, Z-Arg-Arg-NHMec, by cathepsin B was greater for papillary carcinoma than follicular adenoma by eleven-fold, whose activities were completely abolished in the presence of inhibitor, CA-074. 2D SDS-PAGE and 2D immunoblots revealed three isoforms of cathepsin B in follicular adenoma and papillary carcinoma tissues with differential expression. Post-translational detection of cathepsin B isoforms using Pro-Q Diamond phosphoprotein and Pro-Q Emerald glycoprotein gel stains were performed and were both positive in papillary carcinoma. Two isoforms of cathepsin B with similar molecular weights that were positive for phosphorylation in papillary carcinoma were also positive for O-linked N-acetylglucosamine.

## **Chapter 3. Screening for thyroid cancer cell lines with the highest cathepsin B expression**

### **3.1. Introduction**

Originally, the samples intended for this study on the characterization of cathepsin B from benign and malignant thyroid tumors were human tissues. However, as tissues were limited and the amount needed for the purification of the protein was great, we decided to switch to studying cathepsin B from thyroid cell lines instead. We were fortunate to have received five thyroid cell lines from a generous benefactor, Professor Johan R. Lillehaug from the University of Bergen, Norway. Human thyroid cell lines derived from anaplastic carcinomas (CAL-62, 8305C, ARO), papillary carcinoma (B-CPAP) and follicular carcinoma (FTC-133) were shipped from Norway and received by our laboratory.

Among thyroid cancer types, papillary and follicular carcinoma account for 80-90% of all thyroid cancers, followed from medullary carcinoma (5-10%) and the rare anaplastic carcinoma (1-2%). Papillary and follicular carcinomas are referred as well-differentiated thyroid cancers and if detected early, can be treated successfully. Medullary carcinoma can also be treated if the tumor is contained to the local site. On the other hand, anaplastic carcinoma is difficult to control and treat as it is the most aggressive type of thyroid cancer. This part of the report would focus on the study of the expression of cathepsin B in three thyroid cancer cell lines, 8305C, B-CPAP and FTC-133 using one-dimensional and two-dimensional polyacrylamide gel electrophoresis, and immunoblotting.

### **3.2. Cell culture**

RPMI 1640 medium was prepared in the presence of 2.2 g/L  $\text{NaHCO}_3$  and 25 mM HEPES, pH 7.4. DMEM was supplemented with 2.2 g/L of  $\text{NaHCO}_3$ , pH 7.2, whereas Ham's F12 medium was supplemented with 15 mM HEPES and 2 g/L of  $\text{NaHCO}_3$ , pH 7.4. 8305C and B-CPAP cells were thawed and cultured in RPMI 1640 medium with 100 U/mL penicillin, 100 mg/mL streptomycin, 12.5 mg/mL amphotericin B, and 10% fetal bovine serum (FBS) in humidified atmosphere, 95% air, 5%  $\text{CO}_2$  at 37°C. FTC-133 cells were cultured in DMEM:Ham's F12 media (1:1) in the presence of 2 mM glutamine, 100 U/mL penicillin, 100

mg/mL streptomycin, 12.5 mg/mL amphotericin B, and 10% FBS in the same conditions. Images under inverted light microscope for each cell line are shown in Figure 3.1.

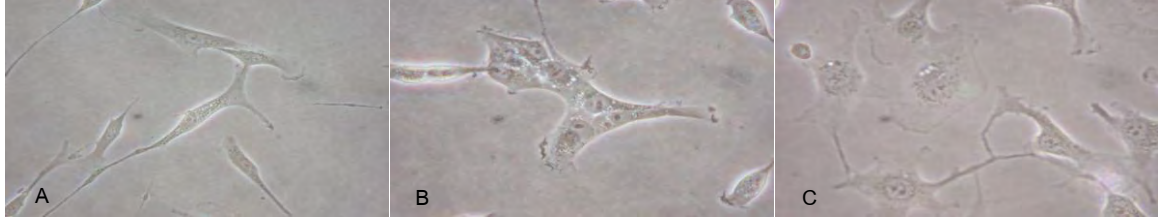


**Figure 3.1. Photographs of thyroid cancer cell lines.** Panels A, B and C represent images of 8305C, B-CPAP and FTC-133 cell lines, respectively, under inverted light microscope with 400x magnification.

Viable cells were counted using trypan blue staining with a hemacytometer. To calculate the doubling time for each cell line, the following equation is used:

$$\text{doubling time} = \frac{(t_2 - t_1) \log 2}{\log N_2 - \log N_1}$$

where  $t_1$  and  $t_2$  are the times (in hours) of the first and second measurements, and  $N_1$  and  $N_2$  are the cell numbers at the first and second measurements, respectively. After counting the number of cells, the doubling times for 8305C, B-CPAP and FTC-133 are 61 hours, 32 hours and 39 hours, respectively.

### 3.3. One-dimensional SDS-PAGE (1-DE)

Cells were harvested at 90-95% confluency, washed three times with 0.25 M sucrose and scraped using cell scraper. Cells were centrifuged, sucrose solution was removed and cell pellets stored at  $-80^{\circ}\text{C}$  for further use. Frozen cells were thawed and incubated with lysis buffer containing 7M urea, 2M thiourea, 4% CHAPS, 2% DTT and 2% ampholine pH 3-10 for one hour at room temperature before sonicating on ice. The cell suspensions were centrifuged at 12,000 rpm for ten minutes at  $4^{\circ}\text{C}$  and the supernatants collected. Protein concentrations were determined using Biorad protein assay using immunoglobulin G as standard. Gels for each cell line can be seen in Figure 3.2.



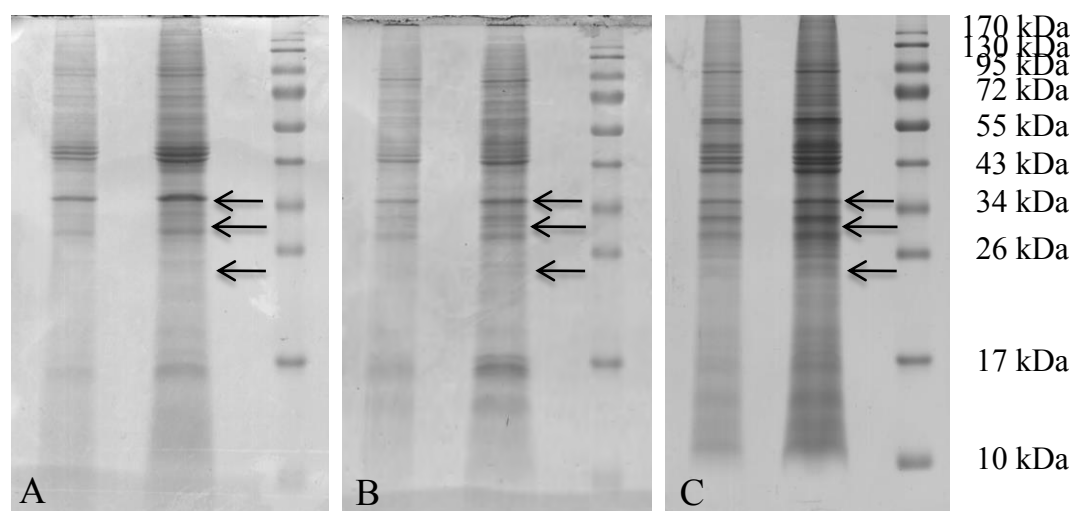


**Figure 3.2. One-dimensional SDS-PAGE of crude cell lysates.** Panels A, B and C represent gels of 8305C, B-CPAP and FTC-133 cell lines, respectively. The first and second lanes in each gel contain 10 mg and 25 mg total protein, respectively, compared to the molecular weight standard in the third lane. Pro-cathepsin B without the signal peptide, active cathepsin B and the heavy chain of cathepsin B have molecular weights of 36 kDa, 27.8 kDa and 22.3 kDa, respectively, as shown by the arrows in each gel.

### 3.4. One-dimensional immunoblotting

In order to optimize the conditions for minimizing nonspecific binding for Western blotting using a recently purchased cathepsin B monoclonal antibody from R&D Systems (no BSA in the formulation), crude lysates from FTC-133 cell line were used and one-dimensional SDS-PAGE performed. After electrophoresis, proteins were transferred to PVDF membranes at 100 V for 1.5 hours at 4°C. Five conditions were tested using the antibody from R&D Systems as compared to that from Calbiochem, as listed below:

Condition 1: block with 10% skim milk, primary antibody (R&D Systems) in 3% BSA, secondary antibody in 10% skim milk

Condition 2: block with 10% skim milk, primary antibody (R&D Systems) in 5% skim milk, secondary antibody in 10% skim milk

Condition 3: block with 10% skim milk, primary antibody (Calbiochem) alone, secondary antibody alone

Condition 4: block with 4% BlockAce, primary antibody (R&D Systems) in 3% BSA, secondary antibody in 5% skim milk

Condition 5: block with 10% skim milk, primary antibody (R&D Systems) alone, secondary antibody in 10% skim milk

Condition 6: block with 10% skim milk, primary antibody (R&D Systems) in 5% skim milk, secondary antibody alone

After blocking for one hour, membranes were probed with 0.25 mg/mL cathepsin B monoclonal antibody from Calbiochem or 4 mg/mL cathepsin B monoclonal antibody from R&D Systems in the absence, presence of 3% BSA or 5% skim milk for 1 hour and repeatedly washed in 20 mM Tris buffered-saline, pH 7.6, containing 0.1% Tween 20. The membranes were then incubated in 1:5000 horseradish peroxidase-conjugated rabbit anti-mouse immunoglobulin or anti-rat immunoglobulin, respectively, in the absence, presence of 5% or 10% skim milk for 1 hour following conditions listed above. After repeated washing, the reaction was developed using the enhanced chemiluminescence (ECL) plus detection system, with high performance film. Condition 4 in Figure 3.3 appeared to have the least nonspecific binding using cathepsin B monoclonal antibody from R&D Systems. There seemed to be different epitopes recognized by the two antibodies from different manufacturers when comparing condition 3 and the other conditions.

Using condition 4, 1D immunoblots using anti-cathepsin B from Calbiochem and R&D Systems were performed for each cell line as shown in Figure 3.4. For both antibodies, 8305C had the highest intensities with the shortest exposure times. Non-specific binding was still present in the 1D immunoblots. Increasing BlockAce from 4% to 10% should help reduce it further and was therefore used for future immunoblots.

### **3.5. Two-dimensional SDS-PAGE (2-DE)**

The supernatants (150 mg total protein) prepared for 1-DE were applied by overnight in-gel rehydration on 7 cm, nonlinear pH 3–10 IPG gel strips and run on IPGphor at 7000 Vh. Focused IPG strips were equilibrated for 10 minutes in a solution (6M urea, 30% glycerol, 1% SDS, 1% DTT in 50mM Tris-HCl buffer, pH 6.8), and then for an additional 10 minutes in the same solution except that DTT was replaced by 2.5% iodoacetamide. The IPG strips were then applied on 12.5% SDS-PAGE in a Hoefer system at 10 mA for 3 hours at room temperature. Gels were then stained with 0.1% Coomassie Blue overnight, destained with 40% methanol, 10% acetic acid, and then scanned (Figure 3.5).

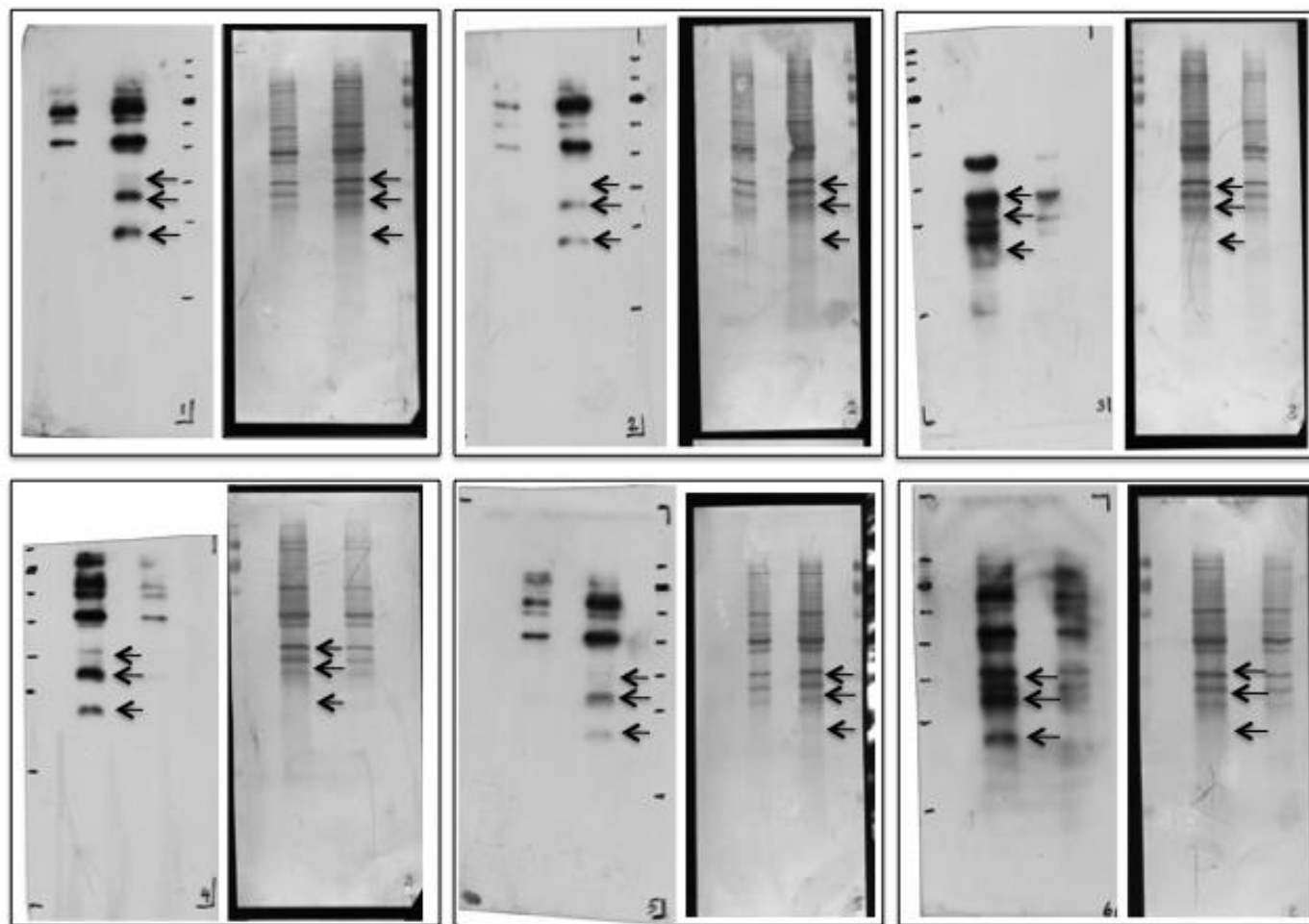


**Figure 3.3. Optimization of conditions for 1D immunoblots of FTC-133 crude lysate.** Panels 1-6 represent conditions 1-6, respectively, as described in the text. The left panel for each condition is the film and the right panel the membrane stained with Coomassie. The film exposure times for conditions 1-6 were 5 minutes, 10 minutes, 10 seconds, 3 minutes, 20 minutes and 5minutes, respectively. The arrows represent procathepsin B, cathepsin B and the heavy chain of cathepsin B from top to bottom.

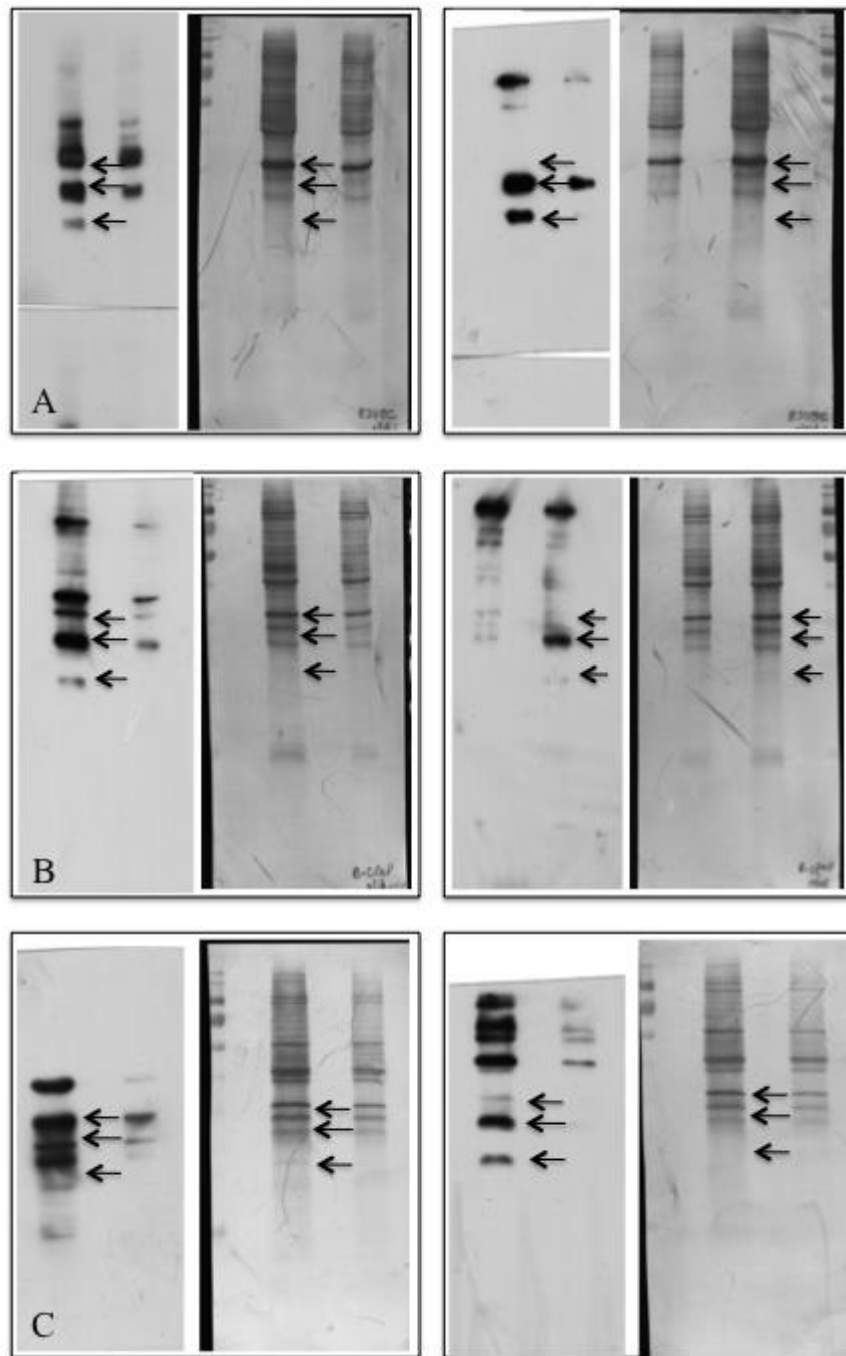


**Figure 3.4. One dimensional immunoblots of three cell lines.** Panels A, B and C represent films (left) and membranes stained with Coomassie blue (right) of 8305C, B-CPAP and FTC-133 cell lines, respectively. Anti-cathepsin B from Calbiochem (left column) and R&D Systems (right column) were used for primary detection. The film exposure times for anti-cathepsin B from Calbiochem and R&D Systems for 8305C were 2 seconds and 1 minute, for B-CPAP were 15 seconds and 5 minutes, and for FTC-133 were 10 seconds and 3 minutes, respectively. The arrows represent procathepsin B, cathepsin B and the heavy chain of cathepsin B from top to bottom.

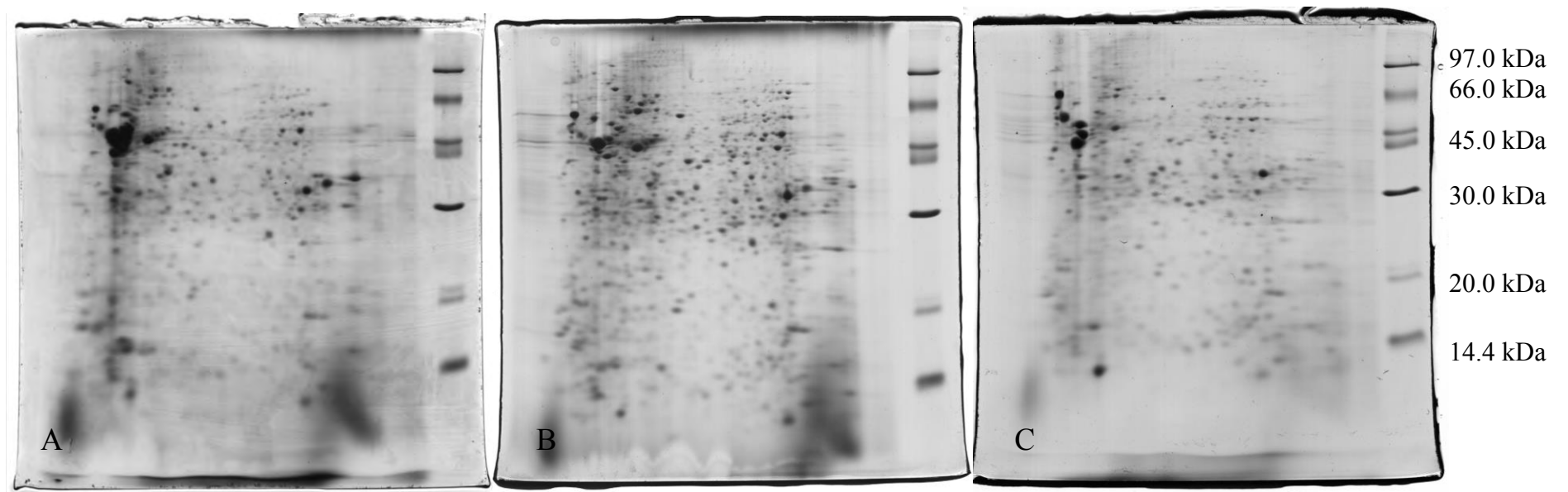


**Figure 3.5. Two-dimensional SDS-PAGE of crude cell lysates.** Panels A, B and C represent gels of 8305C, B-CPAP and FTC-133 cell lines, respectively. The spots corresponding to pro-cathepsin B and cathepsin B are not clearly defined from the 2-DE, thereby requiring immunoblotting using cathepsin B antibodies.

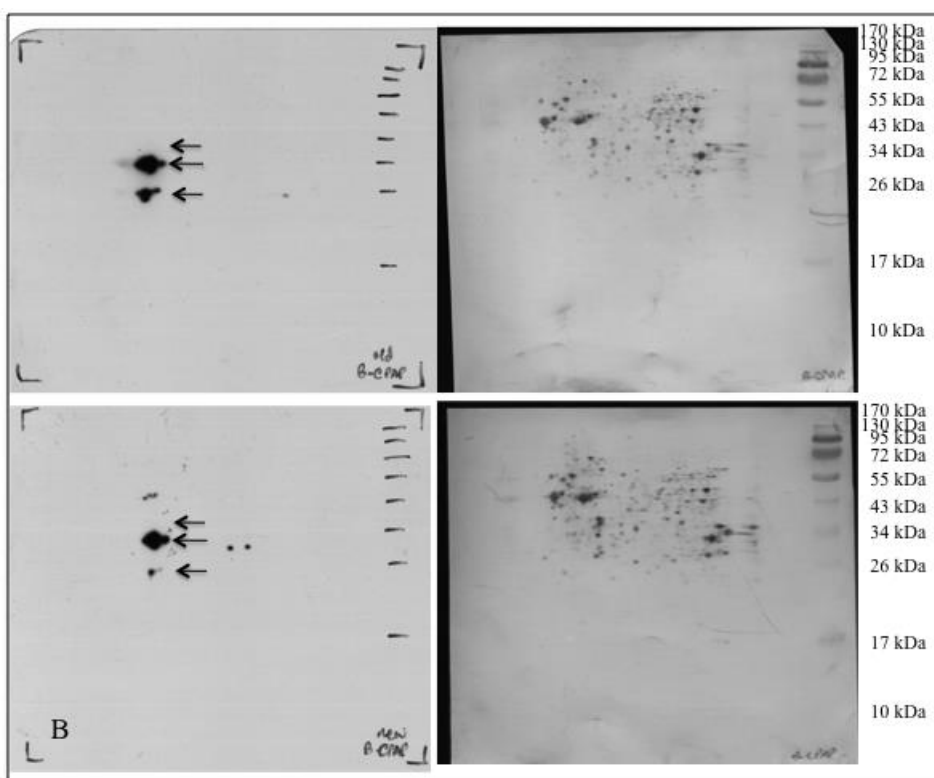
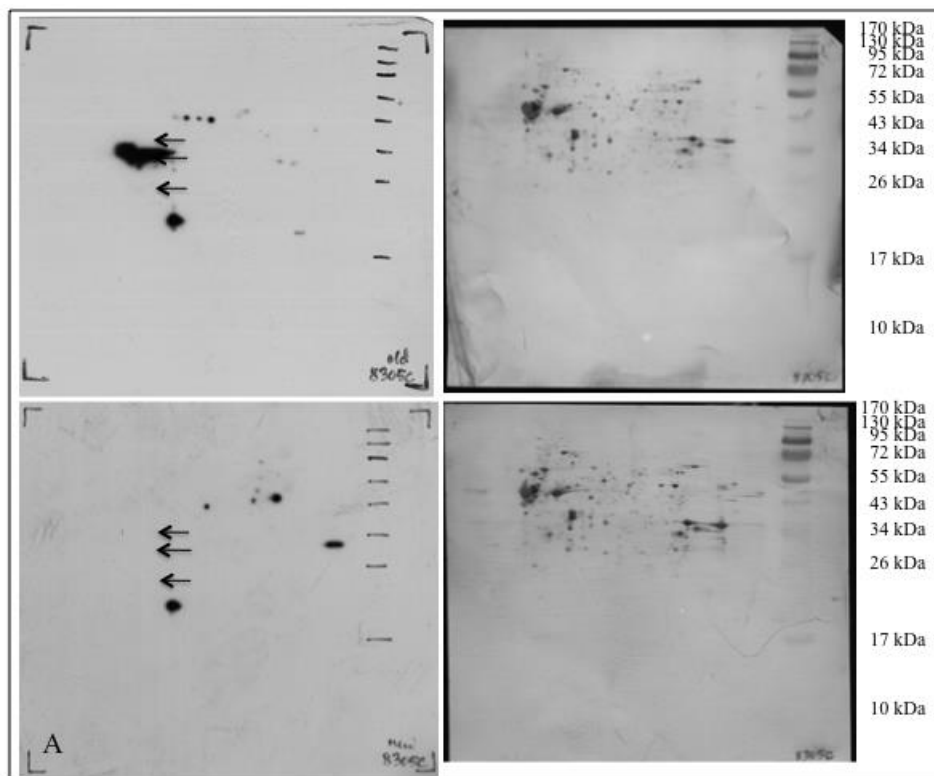
### 3.6. Two-dimensional immunoblotting

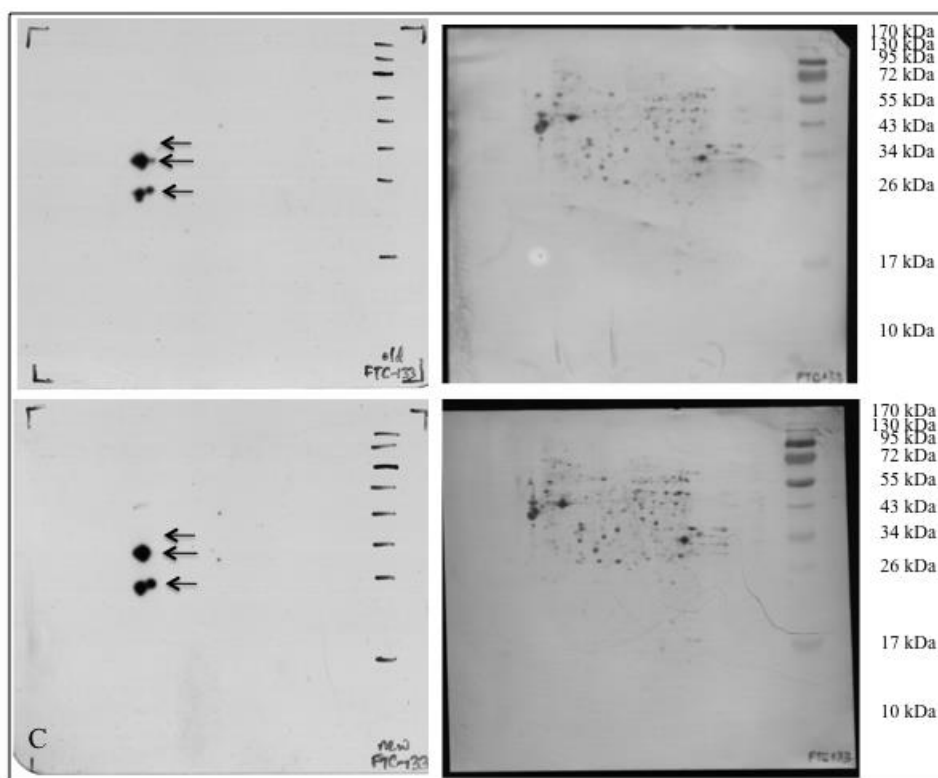
In order to identify the spots in 2-DE corresponding to pro-cathepsin B and cathepsin B, immunoblotting was performed using two different cathepsin B antibodies. After electrophoresis, proteins were transferred to PVDF membranes at 100 V for 1.5 hours at 4°C. After blocking in 10% BlockAce solution for one hour, membranes were probed with 0.25 mg/mL cathepsin B monoclonal antibody from Calbiochem or 4 mg/mL cathepsin B monoclonal antibody from R&D Systems in the presence of 3% BSA for 1 hour and repeatedly washed in 20 mM Tris buffered-saline, pH 7.6, containing 0.1% Tween 20. The membranes were then incubated in 1:5000 horseradish peroxidase-conjugated rabbit anti-mouse immunoglobulin or anti-rat immunoglobulin, respectively in the presence of 5% skim milk for 1 hour. After repeated washing, the reaction was developed using the enhanced chemiluminescence (ECL) plus detection system, with high performance film.

Figure 3.6 shows the immunoblots of each cell line. Interestingly, only active cathepsin B was observed using anti-cathepsin B from Calbiochem, whereas no cathepsin B was observed using anti-cathepsin B from R&D Systems for 8305C (Figure 6A). For B-CPAP and FTC-133, no pro-cathepsin B form (36 kDa) was observed. Active cathepsin B (27.8kDa) and the heavy chain (22.3 kDa) forms were observed with differential expression when comparing B-CPAP and FTC-133, however, no significant differences were observed when using the two antibodies.

### 3.7. Conclusion

One-dimensional immunoblots of each cell line revealed the presence of all isoforms including that of pro-cathepsin B, which were missing in the two-dimensional immunoblots, and optimizing conditions using 1D immunoblots allowed for the decrease in non-specific binding in two-dimensional immunoblots. 2D immunoblots revealed differential expression of active and heavy chain of cathepsin B isoforms in papillary carcinoma (B-CPAP) and follicular carcinoma (FTC-133) cell lines. However, different isoforms of active cathepsin B in anaplastic (8305C) cell line were observed using one monoclonal antibody against cathepsin B from Calbiochem and not from R&D Systems. The intensities in the two-dimensional SDS-PAGE of all forms of cathepsin B were faint, thereby requiring the increased sensitivities gained by immunoblotting. Therefore, it is very unlikely that we can get enough cathepsin B for purification and biochemical and biophysical characterization as planned.





**Figure 3.6. Two-dimensional immunoblots of three cell lines.** Panels A, B and C represent films (left) and membranes stained with Commassie blue (right) of 8305C, B-CPAP and FTC-133 cell lines, respectively using anti-cathepsin B from Calbiochem (top) and R&D Systems (bottom). The film exposure times for 8305C using anti-cathepsin B from Calbiochem and R&D Systems for 8305C were 5 seconds and 5 minutes, for B-CPAP were 5 seconds and 1 minute, and for FTC-133 were 5 seconds and 1 minute, respectively. The arrows represent procathepsin B, cathepsin B and the heavy chain of cathepsin B from top to bottom.



## **Chapter 4. Identification of potential biomarkers for distinguishing between the well-differentiated thyroid cancers**

### **4.1 Introduction**

To date, there is no routine clinical biomarker(s) for thyroid cancer. Malignancy of the thyroid gland is the most common cancer of the endocrine system, with 56,460 estimated new cases in 2012. Among thyroid cancer types, papillary and follicular carcinoma account for 80-90% of all thyroid cancers, followed from medullary carcinoma (5-10%) and the rare anaplastic carcinoma (1-2%). Papillary and follicular carcinomas are referred to as well-differentiated thyroid cancers and if detected early, can be treated successfully. Medullary carcinoma can also be treated if the tumor is contained to the local site. On the other hand, anaplastic carcinoma is difficult to control and treat as it is the most aggressive type of thyroid cancer. Even though cathepsin B has been proposed to be a potential biomarker for thyroid cancer and our results from Chapter 2 and 3 showed that there were differential expression of cathepsin B isoforms in tissues and cell lines, the expression levels of cathepsin B were not too faint to warrant further studies.

Papillary carcinomas are usually diagnosed by fine needle aspiration. However, pathologists agree that the most definitive diagnosis is through histological examination of thyroidectomy specimens. To complicate matters, there is a follicular variant of papillary carcinoma which has low sensitivity using fine needle aspiration biopsy and often misdiagnosed to be follicular adenoma or follicular carcinoma (22). Moreover, the nonmalignant follicular adenoma is impossible to distinguish from follicular carcinoma based on cytology. Therefore, many research groups have tried to identify biomarkers to aid in making an accurate diagnosis. In this study, we aim to use proteomics on papillary (B-CPAP) and follicular (FTC-133) cancer cell lines which could allow for the identification of potential biomarkers for distinguishing between the well-differentiated thyroid cancers.

### **4.2. Cell Culture**

Human thyroid cancer cell line B-CPAP and FTC133 were cultured and maintained in RPMI 1640 and DMEM: F12 (ratio 1:1) media respectively, with 10% fetal bovine serum and

incubated at 37°C in 5% CO<sub>2</sub> under humidified atmosphere. The morphology of FTC-133 cells appears to be more elongated and spindle-like than that of BCPAP, as shown in Figure 4.1.

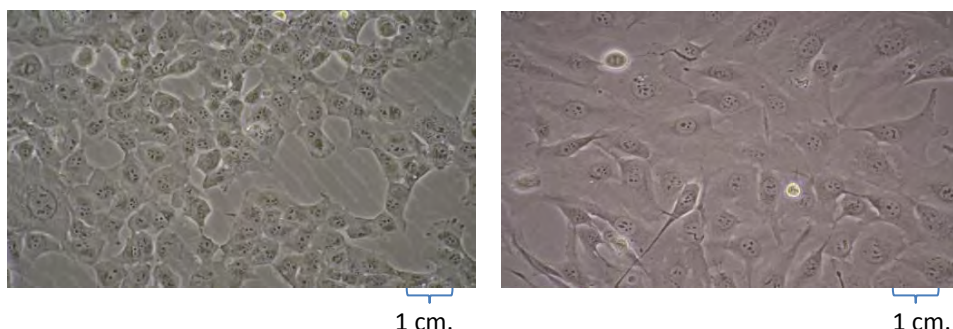


**Figure 4.1. Morphologies of cell lines under phase contrast microscope at 200X.** Left and right panels are B-CPAP and FTC-133 cell line, respectively.

#### **4.3. Cytotoxicity of doxorubicin to BCPAP and FTC133 cell lines**

Cytotoxicity of doxorubicin on BCPAP and FTC-133 cell line were evaluated by MTT assay. Cells were seeded into 96 well-plates at 2000 cells/well and then incubated follow previous descripted overnight. After that, the cells were treated with media contain 0.001, 0.01, 0.1, 0.5, 1, 5, 10, 50 and 100  $\mu$ M doxorubicin and then incubated for forty-eight hours. Media were removed after incubation and 100  $\mu$ L media contained MTT were replaced. Cells were incubated for 2 hours and then formazan crystals were resuspended by 100  $\mu$ L dimethyl sulfoxide (DMSO). Cell viabilities were measured at 550 nm with microplate reader and then inhibitory concentrations at 50% (IC<sub>50</sub>) were determined.

Doxorubicin is one chemotherapeutic drug commonly used to treat metastatic thyroid cancer or recurrent thyroid cancer. We would like to study the effects of doxorubicin on thyroid cancer cell viabilities, especially whether there are differential effects on papillary and follicular carcinomas. The inhibitory concentrations at 50% cell viability for B-CPAP and FTC-133 cell lines are  $0.29 \pm 0.01$   $\mu$ M and  $0.085 \pm 0.018$ , respectively, These results demonstrated that doxorubicin is more effective to treat follicular carcinoma cells than papillary carcinoma cells by approximately three-fold.

#### 4.4. 2-D PAGE and image analysis

B-CPAP and FTC133 were cultured in 75 cm<sup>3</sup> flask until percent confluence rose to around 70-80%. Media was removed and then cells were washed with 3 ml, 0.25 M cold sucrose. Cells were scraped in 450 µL of 0.25 M cold sucrose containing protease inhibitor cocktail (ratio 1: 500, protease inhibitor: sucrose) and then centrifuged at 2500 rpm, 4°C for 10 minutes. Supernatant was removed and then cell pellet was resuspended in lysis buffers containing 5% ampholine (pH 3-10). Samples were incubated at room temperature for 1 hour, sonicated and centrifuged at 12,000 rpm, 4°C, and 10 minutes. Supernatants were collected and protein concentration was determined using Bradford assay. For one-dimensional immunoblots, 10 µg of cell lysate was loaded onto 12.5% SDS-PAGE. For two-dimensional SDS-PAGE, 150 µg of cell lysate was loaded.

One hundred fifty µg of samples were mixed with 75 µL of rehydration buffer contain 2% of IPG buffer, pH 3-10 and then samples were incubated with Immobiline<sup>TM</sup> Drystrips, 7 cm, nonlinear pH 3-10 gradient IPG strips for 16 hours. Isoelectric focusing (IEF) was performed by using Ettan IPGphor 3 (GE healthcare). For the second dimension, strips were equilibrated in two equilibration buffers contain dithiothreitol (DTT) and iodoacetamide (IAA) respectively. Then, proteins were separated on 12.5% SDS-PAGE gel by using PowerPac Basic<sup>TM</sup> (BIO-RAD) apparatus at 10 mA/ gel. Gels were stained by Coomassie blue R-250, scanned by using Labscan 5.0 and ImageMaster 2D Platinum 7.0 program was used for analyzing protein spots. Protein spots with greater than 1.5 fold change and that statistically significant ( $p < 0.05$ ) were selected for further analysis by mass spectrometer.

The two-dimensional SDS-PAGE patterns of B-CPAP and FTC-133 cells are shown in Figure 4.2. There were one hundred and one differential spots that were statistically significant. Fourteen spots and three spots were present in only B-CPAP and FTC-133 cells, respectively. Forty-five spots were increased in B-CPAP and thirty-nine spots were increased in FTC-133 cells.

#### 4.5. In-gel digestion and protein identification

Selected spots were cut from gel and transferred to 1.5 mL tubes. The spots were washed by RO water, excised into small pieces and then destained by 50% acetonitrile (ACN) in 0.1 M NH<sub>4</sub>HCO<sub>3</sub>. After that, gels were reduced by 10 mM DTT at 60°C, 45 minutes

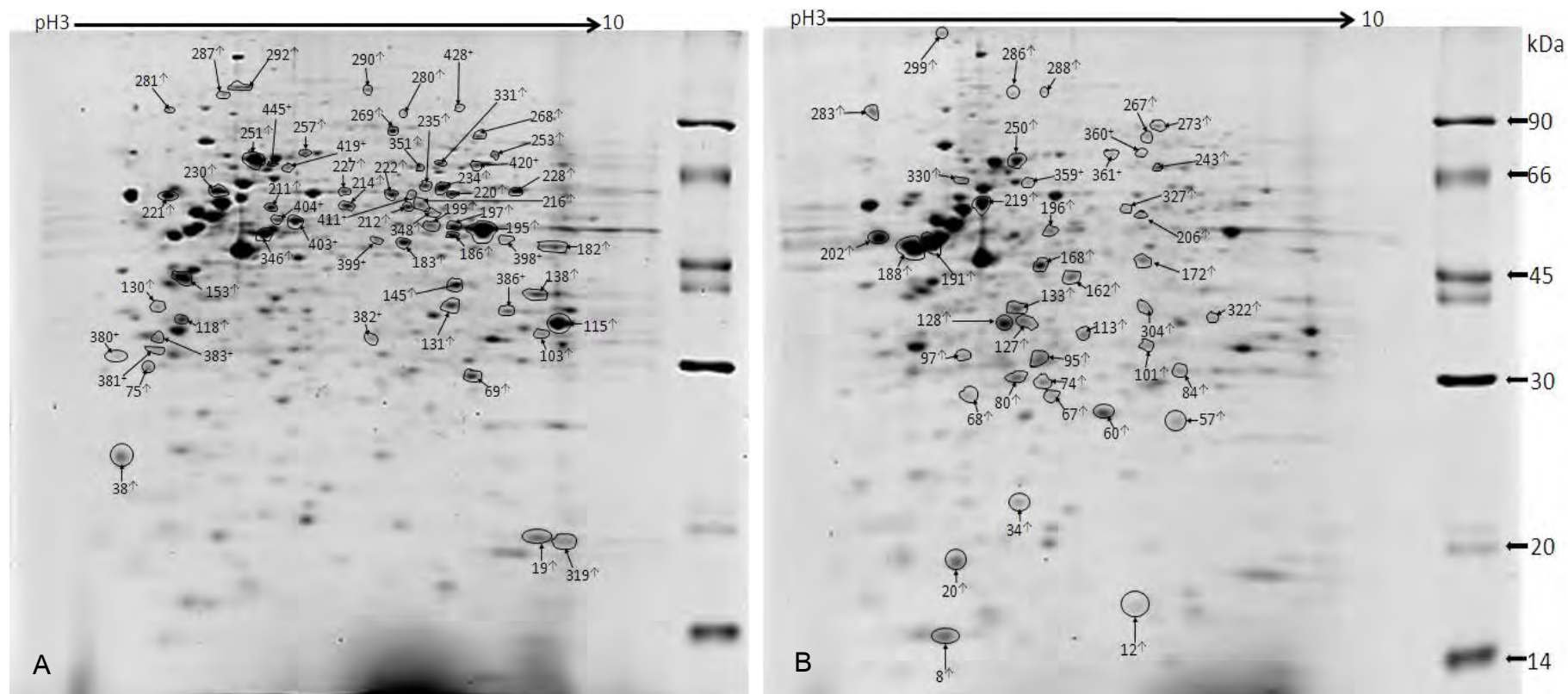


**Figure 4.2. Two-dimensional SDS-PAGE of two well differentiated thyroid cancer cell lines.** Panels A and B are that of B-CPAP and FTC-133 cell lines, respectively. The numbers represent spot numbers and ↑ or + next to the numbers mean spots which have increased percent volume changes or that which appear in only one cell line. Three replicates for each cell line were performed.

and alkylated by 100 mM IAA at room temperature, 30 minutes in dark. Finally, gels were dried and proteins within gels were digested by using trypsin solution that contains 0.01  $\mu$ g trypsin, 0.05 M Tris-HCl pH 8.5, 10% ACN and 1 mM  $\text{CaCl}_2$ . Gels were incubated at 37°C, overnight and then supernatants were collected for protein identification by LC-MS/MS.

The selected protein spots were identified by using nanoflow-LC coupled to an amazon speed ion trap mass spectrometer. Tryptic peptides were concentrated and desalted using 75  $\mu$ m id  $\times$  100 mm  $\text{C}_{18}$  EASY-nLC<sup>TM</sup> column (Thermo Scientific, USA). The peptides were eluted by 0.1% formic acid in water (solution A) and 0.1% formic acid in ACN (solution B), respectively and then 6  $\mu$ L of sample was injected into nano-LC system and then separation at a flow rate 0.0005 mL/minute for 30 minutes using the gradient: 0 min 95% A, 20 min 60% A, 20.5 min 5% A, 29 min 5% A, and 29.5 min 95% A. For mass analysis, CaptiveSpray<sup>TM</sup> was performed at 1.0 sec atomic scan rate with 0.1 sec inter delay and parent mass peak with range 50 to 3000  $m/z$  were selected for MS/MS analysis. Collision energy was fixed at 1300 V. Bruker Compass 1.4 software was used for processing MS/MS data and converting to .mgf file.

Proteins were identified by using MASCOT search engine ([www.matrixscience.com](http://www.matrixscience.com)). Parameters were defined as follows: Database, NCBI; Taxonomy, *Homo sapiens*; Enzyme, trypsin; One missed cleavage allowed; Fixed modification, carbamidomethyl (C); Variable modification, phospho (ST) and phospho (Y); Peptide and MS/MS fragment ion mass tolerance, 1.2 and 0.6 Da; Peptide charge, 1+, 2+ and 3+. Proteins with molecular weight and pI consistent to gel spots with MASCOT score > 25 using  $p$ -value  $\leq$  0.05 were considered as positively identified.

Forty spots, appearing in only one cell line and that with highest fold changes between the two cell lines, were selected for digestion and analysis by LC/MS/MS. Table 4.1 and 4.2 list the proteins identified from LC/MS/MS for B-CPAP and FTC-133 cell line, respectively. Based on the function of the proteins identified, those proteins can be classified into twelve groups for B-CPAP and seven groups for FTC-133, as shown in Figure 4.3. Five groups were common to both cell lines, which include proteins involved in structure, cell proliferation, stress response, cell migration and anti-apoptosis.

**Table 4.1. Identified proteins based on tryptic digestion and LC/MS/MS for B-CPAP cell line**

Spot no.	Accession no.	Description	MW/pI	Peptide match	% Coverage	Score	Sequence	Functions	Fold change	Alternative names
38	gi 9257073	Co-Chaperone P23	15146 /5.09	2	12	68	R.SILCCLR.K K.DVNVNFEK.S	Molecular chaperone that localizes to genomic response elements in a hormone-dependent manner and disrupts receptor-mediated transcriptional activation.	1.4940	- Prostaglandin E synthase 3 - Cytosolic prostaglandin E2 synthase(cPGES) - Hsp90 co-chaperone - Progesterone receptor complex p23 - Telomerase-binding protein p23
69	gi 4507645	Triosephosphate isomerase isoform 1	26938 /6.45	12	55	548	K.VVFEQTK.V K.FFVGGNWK.M K.IAVAAQNCYK.V K.SNVSDAVAQSTR.I R.IIYGGSVTGATCK.E K.QSLGELIGTLNAAK.V R.HVFGESDELIGQK.V K.TATPQQAQEVHEK.L K.DCGATWVVLGHSER.R K.VVLAYEPVWAIGTGK.T R.RHVFGESDELIGQK.V K.VAHALAEGLGVIACIGEK.L	Glycolysis	1.3202	- TPI

**Table 4.1. Identified proteins based on tryptic digestion and LC/MS/MS for B-CPAP cell line (continued)**

Spot no.	Accession no.	Description	MW/pI	Peptide match	% Coverage	Score	Sequence	Functions	Fold change	Alternative names
115	gi 31645	Glyceraldehyde-3-phosphate dehydrogenase	36202 /8.26	9	30	311	K.VGVNGFGR.I K.QASEGPLK.G R.VVDLMAHMASK.E R.GALQNIIPASTGAAK.A R.GALQNIIPASTGAAK.A R.VPTANVSVDLTCR.L K.LVINGNPITIFQER.D K.LISWYDNEFGYSNR.V K.IISNASCTTNCLAPLAK.V	Glycolysis	2.2176	- GADPH
131	gi 14043145	LASP1 protein	36789 /8.92	4	10	127	K.YHEEFK.S R.DSQDGSSYR.R K.TQDQISNIK.Y K.QQSELQSQVR.Y	Plays an important role in the regulation of dynamic actin-based, cytoskeletal activities that relate to cancer cell invasion and migration	2.1803	- LIM and SH3 domain protein 1 - Metastatic lymph node gene 50 protein(MLN50)
145	gi 332801090	Heterogeneous nuclear ribonucleoprotein D-like isoform b	40187 /9.98	4	7	159	K.DLTEYLSR.F R.FGEVVDCTIK.T R.GFGFVLFK.D R.GFGFVLFK.D	Play role in apoptosis	1.7013	- hnRNP DL - JKT41-binding protein - AU-rich element RNA-binding factor - Protein laAUF1
153	gi 825671	B23 nucleophosmin	31090 /4.71	2	5	62	K.MQASIEK.G K.GPSSVEDIK.A	Involved in diverse cellular processes such as ribosome biogenesis, centrosome duplication, protein chaperoning, histone assembly, cell proliferation, and anti-apoptosis.	1.2298	- Nucleophosmin - Nucleolar phosphoprotein B23 - Nucleolar protein NO38 - Numatrin

**Table 4.1. Identified proteins based on tryptic digestion and LC/MS/MS for B-CPAP cell line (continued)**

Spot no.	Accession no.	Description	MW/pI	Peptide match	% Coverage	Score	Sequence	Functions	Fold change	Alternative names
195	gi 4503571	Alpha-enolase isoform 1	47481 /7.01	19	41	657	K.YDLDFK.S K.YDLDFK.S K.YNQLLR.I K.TIAPALVSK.K R.IEEELGSK.A K.LNVTEQEK.I K.SCNCLLLK.V K.SCNCLLLK.V K.KLVNTEQEK.I R.IGAEVYHNLK.N K.LMIEMDGTENK.S R.YISPDQLADLYK.S K.VVIGMDVAASEFFR.S K.LAQANGWGMVSHR.S + Phospho (ST) K.VNQIGSVTESLQACK.L K.LAMQEFMILPVGAANFR.E K.DATNVGDEGGFAPNILENK.E K.FTASAGIQVVGDDLTVTNPK.R	Play role in glycolysis, cell growth, hypoxia tolerance, Allergic response and may be tumor suppressor	1.6857	- 2-phospho-D-glycerate hydro-lyase - C-myc promoter-binding protein - Enolase 1 - MBP-1 - MPB-1 - Non-neural enolase (NNE) - Phosphopyruvate hydratase - Plasminogen-binding protein
222	gi 5453603	T-complex protein 1 subunit beta isoform 1	57794 /6.01	7	13	210	K.VLVDMSR.V R.EAESLIAK.K K.LAVEAVLR.L K.NIGVDNPAK.V K.EAVAMESYAK.A R.AAHSEGNTTAGLDMR.E R.EALLSSAVDHGSDEVK.F	Part of the BBS/CCT complex may play a role in the assembly of BBSome, a complex involved in ciliogenesis regulating transports vesicles to the cilia. Known to play a role, in vitro, in the folding of actin and tubulin.	1.9235	- TCP-1 beta - CCT-beta



**Table 4.1. Identified proteins based on tryptic digestion and LC/MS/MS for B-CPAP cell line (continued)**

Spot no.	Accession no.	Description	MW/pI	Peptide match	% Coverage	Score	Sequence	Functions	Fold change	Alternative names
228	gi 35505	Pyruvate kinase	58411 /7.58	17	30	714	R.APIIAVTR.N R.MQHLIAR.E R.GIFPVLCK.D R.VNFAMNVGK.A K.GSGTAEVELK.K K.GDYPLEAVR.M K.GSGTAEVELKK.G R.GDLGIEIPAEK.V R.LDIDSPPIAR.N K.CCSGAIIVLTK.S R.NTGIICTIGPASR.S K.IYVDDGLISLQVK.Q K.GVNLPGAAVDLPVSEK.D K.KGVNLPGAAVDLPVSEK.D R.AGKPVICATQMLESMIK.K R.EAEAAIYHLQLFEELR.R	Glycolysis	1.7031	- PK

**Table 4.1. Identified proteins based on tryptic digestion and LC/MS/MS for B-CPAP cell line (continued)**

Spot no.	Accession no.	Description	MW/pI	Peptide match	% Coverage	Score	Sequence	Functions	Fold change	Alternative names
234	gi 5803181	Stress-induced-phosphoprotein 1	63227 /6.40	19	29	704	R.TPDVLKK.C K.AAALEAMK.D K.DFDTALK.H R.IGNSYFK.E R.TYEEGLK.H K.AMDVYQK.A K.HYTEAIK.R K.ELGNDAYK.K K.GDYPQAMK.H R.LILEQMVK.D K.AAALEFLNR.F K.ALDLDSSCK.E R.TLLSDPTYR.E R.CMMAQYNR.H K.LLEFQLALK.D K.LMDVGLIAIR.- K.DPQALSEHLK.N K.YKDAIHFNK.S K.LDPHNHVLYSNR.S	Mediates the association of the molecular chaperones HSC70 and HSP90	3.1749	- ST11 - Hsc70/Hsp90-organizing protein(HOP) - Renal carcinoma antigen NY-REN-11 - Transformation-sensitive protein IEF SSP 3521

**Table 4.1. Identified proteins based on tryptic digestion and LC/MS/MS for B-CPAP cell line (continued)**

Spot no.	Accession no.	Description	MW/pI	Peptide match	% Coverage	Score	Sequence	Functions	Fold change	Alternative names
251	gij5729877	Heat shock cognate 71 kDa protein isoform 1	71082 /5.37	13	19	472	K.ITITNDK.G R.GTLDPVEK.A K.VCNPIITK.L K.EIAEAYLGK.T K.LLQDFFNGK.E K.FELTGIPPAPR.G K.DAGTIAGLNVL.R K.VEIANDQGNR.T R.MVNHFAIEFK.R K.MKEIAEAYLGK.T R.RFDDAVVQSDMK.H R.ARFEELNADLFR.G K.SQIHDIIVLVGGSTR.I	Acts as a repressor of transcriptional activation and response to cell stress	1.6498	- Heat shock 70 kDa protein 8
380	gij4507953	14-3-3 protein zeta/delta	27899 /4.73	3	12	121	R.NLLSVAYK.N R.YLAEVAAGDDKK.G K.DSTLIMQLLR.D	May play role in cell survival.	Present	- Protein kinase C inhibitor protein 1 - KCIP-1
381	gij350610434	14-3-3 Sigma	26584 /4.90	4	14	150	R.VLSSIEQK.S R.NLLSVAYK.N R.YEDMAAFMK.G K.DSTLIMQLLR.D	Involved in diverse cellular processes protein such as cell cycle arrest.	Present	- Epithelial cell marker protein 1 - Stratifin
	gij380765197	Tyrosine 3-Monooxygenase	28373 /4.80	4	10	145	R.VISSIEQK.T R.NLLSVAYK.N K.DSTLIMQLLR.D K.DSTLIFQLLR.D	Plays an important role in the physiology of adrenergic neurons		- Tyrosine 3-hydroxylase

**Table 4.1. Identified proteins based on tryptic digestion and LC/MS/MS for B-CPAP cell line (continued)**

Spot no.	Accession no.	Description	MW/pI	Peptide match	% Coverage	Score	Sequence	Functions	Fold change	Alternative names
382	gi 4758484	Glutathione S-transferase omega-1 isoform 1	27833 /6.23	5	17	198	K.LEEVLTNK.K K.MILELFSK.V K.VPSLVGSFIR.S R.HEVININLK.N K.NKPEWFFK.K	Exhibits glutathione-dependent thiol transferase, dehydroascorbate reductase, S-(phenacyl)glutathione reductase and glutathione S-transferase activity.	Present	- Glutathione -dependent dehydroascorbate reductase - Monomethylarsonic acid reductase - S-(Phenacyl)glutathione reductase
	gi 704416	Elongation factor Tu	49851 /7.70	4	9	94	K.TTLTAAITK.I R.GTVVTGTLER.G R.TVVTGIEMFHK.S R.QIGVEHVVVYVVK.A	This protein promotes the GTP-dependent binding of aminoacyl-tRNA to the A-site of ribosomes during protein biosynthesis		- P43
383	gi 5803225	14-3-3 protein epsilon [Homo sapiens]	29326/4.63	7	29	260	R.NLLSVAYK.N R.IISSIEQK.E R.EDLVYQAK.L K.DSTLIMQLLR.D K.EAAENSLVAYK.A R.YLAEFATGNDRK.E K.AASDIAMTELPPTHPIR.L	May involved cell survival and anti-apoptosis	Present	

**Table 4.1. Identified proteins based on tryptic digestion and LC/MS/MS for B-CPAP cell line (continued)**

Spot no.	Accession no.	Description	MW/pI	Peptide match	% Coverage	Score	Sequence	Functions	Fold change	Alternative names
386	gij114794644	Annexin A2	35448 /8.21	10	33	470	R.SEVDMLK.I R.DLYDAGVK.R K.WISIMTER.S R.DALNIETAIK.T R.QDIAFAYQR.R K.TPAQYDASELK.A K.DIISDTSGDFR.K R.TNQELQEINR.V K.GVDEVTVNLTNR.S K.SALSGHLETVILGLLK.T	Calcium-regulated membrane-binding protein whose affinity for calcium is greatly enhanced by anionic phospholipids. It binds two calcium ions with high affinity. May be involved in heat-stress response and cell invasion and migration	Present	- Annexin II - Calpactin I heavy chain - Chromobindin-8 - Lipocortin II - Placental anticoagulant protein IV - p36
398	gij870743	Heterogeneous nuclear ribonucleoprotein D	30523 /9.20	3	6	110	R.GFGFVLFK.E R.GFGFVLFK.E K.FGEVVDCTLK.L	May play role in cell proliferation	Present	- hnRNP D - AU-rich element RNA-binding protein 1
399	gij4099506	erbB3 binding protein EBP1	38320 /7.15	5	13	227	K.ALLQSSASR.K K.SDQDYILK.E R.AFFSEVER.R K.EGEFVAQFK.F K.AAHLCAEAALR.L	Binds and is activated by neuregulins and NTAK. May play role in cell proliferation	Present	- Proto-oncogene-like protein c-ErbB-3 - Tyrosine kinase-type cell surface receptor HER3
	gij2697005	Cell cycle protein p38-2G4 homolog	44127 /6.13	5	11	226	K.SDQDYILK.E K.AAHLCAEAALR.L R.AFFSEVER.R K.EGEFVAQFK.F K.ALLQSSASR.K	Seems be involved in growth regulation.		- Cell cycle protein p38-2G4 homolog - ErbB3-binding protein 1

**Table 4.1. Identified proteins based on tryptic digestion and LC/MS/MS for B-CPAP cell line (continued)**

Spot no.	Accession no.	Description	MW/pI	Peptide match	% Coverage	Score	Sequence	Functions	Fold change	Alternative names
403	gil181573	Cytokeratin 8	53529 /5.52	18	31	714	K.FASFIDK.V R.FLEQQNK.M K.LLEGEESR.L K.TEISEMNR.N R.LQAEIEGLK.G K.WSLLQQQK.T K.AQYEDIANR.S K.DVDEAYMNK.V K.LSELEAALQR.A K.YEELQSLAGK.H R.EYQELMNVK.L R.AEAESMYQIK.Y K.LVSESSDVLPK.- R.TKTEISEMNR.N R.SLDMSIIAEVK.A R.ASLEAAIADAEQR.G R.ASLEAAIADAEQR.G K.LALDIEIATYRK.L	Together with KRT19, helps to link the contractile apparatus to dystrophin at the costameres of striated muscle	Present	- CK8
	gil4504169	Glutathione synthetase	52523 /5.67	4	6	151	R.HVLSVLSK.T R.ALAEGVLLR.T R.ASYILMEK.I R.TFEDISEK.G	Glutathione biosynthesis		

**Table 4.1. Identified proteins based on tryptic digestion and LC/MS/MS for B-CPAP cell line (continued)**

Spot no.	Accession no.	Description	MW/pI	Peptide match	% Coverage	Score	Sequence	Functions	Fold change	Alternative names
404	gi 181573	Cytokeratin 8	53529 /5.52	14	26	562	K.FASFIDK.V R.FLEQQNK.M K.LLEGEESR.L K.TEISEMNR.N R.LQAEIEGLK.G K.WSLLQQQK.T R.QLYEEEIR.E K.DVDEAYMNK.V K.LSELEAALQR.A K.YEELQSLAGK.H R.EYQELMNVK.L K.LVSESSDVLPK.- R.ASLEAAIADAEQR.G R.LESGMQNMSIHTK.T	Together with KRT19, helps to link the contractile apparatus to dystrophin at the costameres of striated muscle	Present	- CK8
411	gi 14495609	CTP synthase	67358 /6.02	7	11	328	K.IQAIWAR.N R.RLDLPIER.Q K.IYQYVINK.E K.FSDSYASVIK.A R.CSNPLDTSVK.E K.GIIASSVGTILK.S K.ALEHSALAINHK.L	Catalyzes the ATP-dependent amination of UTP to CTP with either L-glutamine or ammonia as the source of nitrogen	Present	- CTP synthetase 1 - UTP--ammonia ligase 1
419	gi 23397696	Copine-1 isoform a	59649 /5.52	7	11	236	R.QALPQVR.L K.TLQLEYR.F K.NNLNPTWK.R R.NCSSPEFSK.T R.FGIYDIDNK.T R.DIVQFVPYR.R R.GTITVSAQELK.D	May function in membrane trafficking. Exhibits calcium-dependent phospholipid binding properties	Present	

**Table 4.1. Identified proteins based on tryptic digestion and LC/MS/MS for B-CPAP cell line (continued)**

Spot no.	Accession no.	Description	MW/pI	Peptide match	% Coverage	Score	Sequence	Functions	Fold change	Alternative names
420	gi 11527777	Heterogeneous nuclear ribonucleoprotein L	64617 /8.49	4	6	137	K.TPASPVVHIR.G R.AITHLNNFMFGQK.L K.LNVCVSK.Q K.LCFSTAQHAS.-	This protein is a component of the heterogeneous nuclear ribonucleoprotein (hnRNP) complexes which provide the substrate for the processing events that pre-mRNAs undergo before becoming functional, translatable mRNAs in the cytoplasm. And may relate to angiogenesis	Present	- hnRNP L
428	gi 4503483	Elongation factor 2	96246 /6.41	3	3	128	K.FSVSPVVR.V M.VNFTVDQIR.A R.VFSGLVSTGLK.V	Play role in cell proliferation	Present	- EF-2
445	gi 4529892	Heat shock 70 kDa protein 2	70267 /5.48	6	8	199	K.DNNLLGR.F K.ITITNDK.G K.SAVEDEGLK.G K.LLQDFFNDR.D R.LVNHFVEEFKR.K K.HWPFQVINDGDKPK.V	involved stress response	Present	- HSP70-2 - Heat shock 70 kDa protein 1A/1B - Heat shock 70 kDa protein 1 (HSP70-1)



**Table 4.2. Identified proteins based on tryptic digestion and LC/MS/MS for FTC-133 cell line**

Spot no.	Accession no.	Description	MW/pI	Peptide match	% Coverage	Score	Sequence	Functions	Fold change	Alternative names
8	gi 28336	Beta-actin	42128 /5.22	5	16	260	K.AGFAGDDAPR.A R.GYSFTTTAER.E K.EITALAPSTMK.I K.DSYVGDEAQS.K R.VAPEEHPVLLTEAPLNPK.A	Actins are highly conserved proteins that are involved in various types of cell motility and are ubiquitously expressed in all eukaryotic cells	3.1521	
20	gi 4503545	Eukaryotic translation initiation factor 5A-1 isoform B	17049 /5.08	5	25	183	R.LPEGDLGK.E K.IVEMSTSK.T R.KNGFVVLK.G K.VHLVGIDIFTGK.K R.EDLRLPEGDLGK.E	mRNA-binding protein involved in translation elongation. Involved in cell survival actin dynamics and cell cycle progression, mRNA decay and probably in a pathway involved in stress response and maintenance of cell wall integrity.	1.3804	- Eukaryotic initiation factor 5A isoform 1 (eIF-5A) - Rev-binding factor - eIF-4D
60	gi 4504517	Heat shock protein beta-1	22826 /5.98	8	36	358	K.DGVVEITGK.H R.AQLGGPEAAK.S R.GPSWDPFR.D R.QLSSGVSEIR.H R.QDEHGYISR.C K.TKDGVEITGK.H R.LFDQAFGLPR.L R.VSLDVNHFAPELTVK.T	Involved in stress resistance and actin organization	3.9332	- HspB1 - 28 kDa heat shock protein - Estrogen-regulated 24 kDa protein - Heat shock 27 kDa protein - Stress-responsive protein 27

**Table 4.2. Identified proteins based on tryptic digestion and LC/MS/MS for FTC-133 cell line (continued)**

Spot no.	Accession no.	Description	MW/pI	Peptide match	% Coverage	Score	Sequence	Functions	Fold change	Alternative names
68	gi 4502101	Annexin A1	38918 /6.57	2	4	76	R.NALLSLAK.G R.ALYEAGER.R	Calcium/phospholipid-binding protein which promotes membrane fusion and is involved in exocytosis. This protein regulates phospholipase A2 activity.	1.6415	- Annexin I - Calpactin II - Chromobindin-9 - Lipocortin I - Phospholipase A2 inhibitory protein - p35
80	gi 4505773	Prohibitin	29843 /5.57	7	27	292	K.EFTEAVEAK.Q K.QVAQQEAER.A K.AAIISAEGDSK.A R.FDAGELITQR.E K.DLQNVNITLR.I R.VLPSITTEILK.S R.KLEAAEDIAYQLSR.S	Prohibitin inhibits DNA synthesis. It has a role in regulating proliferation. May play a role in regulating mitochondrial respiration activity and in aging.	1.7887	- PHB
128	gi 4504981	Galectin-1	15048 /5.34	5	33	132	K.SFVLNLGK.D K.DGGAWGTEQR.E K.DSNNLCLHFNPR.F K.DSNNLCLHFNPR.F R.FNAHGDANTIVCNSK.D	May regulate apoptosis, cell proliferation and cell differentiation. Binds beta-galactoside and a wide array of complex carbohydrates. Inhibits CD45 protein phosphatase activity and therefore the dephosphorylation of Lyn kinase	1.7512	- HLBP14 - Beta-galactoside-binding lectin L-14-I - Galaptin - HBL,HDL - Putative MAPK-activating protein PM12

**Table 4.2. Identified proteins based on tryptic digestion and LC/MS/MS for FTC-133 cell line (continued)**

Spot no.	Accession no.	Description	MW/pI	Peptide match	% Coverage	Score	Sequence	Functions	Fold change	Alternative names
168	gil18088719	Beta tubulin	50096 /4.75	10	22	397	K.IREEYPDR.I R.FPGQLNADLR.K K.LAVNMVPPFR.L R.FPGQLNADLRK.L R.ISVYYNEATGGK.Y R.IMNTFSVVPSPK.V R.LHFFMPGFAPLTSR.G R.ALTVPILTQQVFDAK.N K.GHYTEGAELVDSVLDVVR.K	Tubulin is the major constituent of microtubules. It binds two moles of GTP, one at an exchangeable site on the beta chain and one at a non-exchangeable site on the alpha chain.	1.2893	
191	gil340219	Vimentin	53738 /5.03	19	34	733	R.FANYIDK.V K.GTNESLER.Q K.LLEGEESR.I R.QQYESVAAK.N K.LQEEMLQR.E R.QVDQLTNDK.A R.DNLAEDIMR.L K.FADLSEAANR.N K.VELQELNDR.F R.LQDEIQNMK.E R.EYQDLLNVK.M K.ILLAELEQLK.G R.RQVDQLTNDK.A R.LGDLYEEEMR.E R.EEAENTLQSFR.Q R.KVESLQEEIAFLK.K K.ILLAELEQLKGQK.S R.ETNLDLPLVDTHSK.R	Vimentins are class-III intermediate filaments found in various non-epithelial cells, especially mesenchymal cells. Vimentin is attached to the nucleus, endoplasmic reticulum, and mitochondria, either laterally or terminally.	2.7895	- VIM

**Table 4.2. Identified proteins based on tryptic digestion and LC/MS/MS for FTC-133 cell line (continued)**

Spot no.	Accession no.	Description	MW/pI	Peptide match	% Coverage	Score	Sequence	Functions	Fold change	Alternative names
219	gi 4505257	Moesin	67892 /6.08	5	8	209	K.EALLQASR.D R.ISQLEMAR.Q R.ALELEQER.K K.TANDMIHAENMR.L R.RKPDITIEVQQMK.A	Probably involved in connections of major cytoskeletal structures to the plasma membrane. May inhibit herpes simplex virus 1 infection at an early stage	1.5860	- Membrane-organizing extension spike protein
327	gi 1263008	Aldehyde dehydrogenase	57637 /6.41	9	14	335	R.ELGEDGLK.A K.IEEVVER.A R.YFAGWADK.W K.KIEEVVER.A R.YGLAAAVFTR.D R.VLGYIQLGQK.E R.LLNLLADLVER.D R.YFAGWADKWHGK.T K.VAFTGSTEVGHLIQK.A	Catalyzes the oxidation of long-chain aliphatic aldehydes to fatty acids that involved fatty acid synthesis. May act as anti-oxidant	3.7081	- ALDH

**Table 4.2. Identified proteins based on tryptic digestion and LC/MS/MS for FTC-133 cell line (continued)**

Spot no.	Accession no.	Description	MW/pI	Peptide match	% Coverage	Score	Sequence	Functions	Fold change	Alternative names
359	gi 119604041	Staphylococcal nuclease domain containing 1, isoform CRA_a	59542 /5.71	10	19	350	K.GDVGLGLVK.E K.VHF TAER.S R.TDAVDSVVR.D K.SLLSAEEAAK.Q R.VADISGDTQK.A K.QFLPFLQR.A K.FVDGEWYR.A R.LGTLSPAFSTR.V R.SSHYDELLAAEAR.A R.NDIASHPPVEGSYAPR.R	Functions as a bridging factor between STAT6 and the basal transcription factor. Plays a role in PIM1 regulation of MYB activity. Functions as a transcriptional coactivator for the Epstein-Barr virus nuclear antigen 2 (EBNA2)	Present	- 100 kDa coactivator - EBNA2 coactivator p100 - Tudor domain-containing protein 11 - p100 co-activator
	gi 460789	Transformation upregulated nuclear protein	51325 /5.13	2	5	71	K.DLAGSIIGK.G R.LLIHQSLAGGIIGVK.G	Likely to play a role in the nuclear metabolism of hnRNAs. Plays an important role in p53/TP53 response to DNA damage, and involve cell proliferation.		- Heterogeneous nuclear ribonucleoprotein K - TUNP
360	gi 1536909	ULIP	62279 /6.04	3	4	129	K.IFNLYPR.K K.QEVQNLIK.D R.GAPLVVICQGK.I	Necessary for signaling by class 3 semaphorins and subsequent remodeling of the cytoskeleton. Plays a role in axon guidance, neuronal growth cone collapse and cell migration	Present	- Unc-33-like phosphoprotein 1 - Dihydropyrimidinase-related protein 3 - Collapsin response mediator protein 4

**Table 4.2. Identified proteins based on tryptic digestion and LC/MS/MS for FTC-133 cell line (continued)**

Spot no.	Accession no.	Description	MW/pI	Peptide match	% Coverage	Score	Sequence	Functions	Fold change	Alternative names
361	gi 1536909	ULIP	62279 /6.04	6	7	284	R.MSVIWDK.A K.IFNLYPR.K K.QEVQNLIK.D K.EVLQNLGPK.D K.SAADLISQAR.K R.GAPLVVICQGK.I	Necessary for signaling by class 3 semaphorins and subsequent remodeling of the cytoskeleton. Plays a role in axon guidance, neuronal growth cone collapse and cell migration	Present	- Unc-33-like phosphoprotein 1 - Dihydropyrimidinase-related protein 3 - Collapsin response mediator protein 4

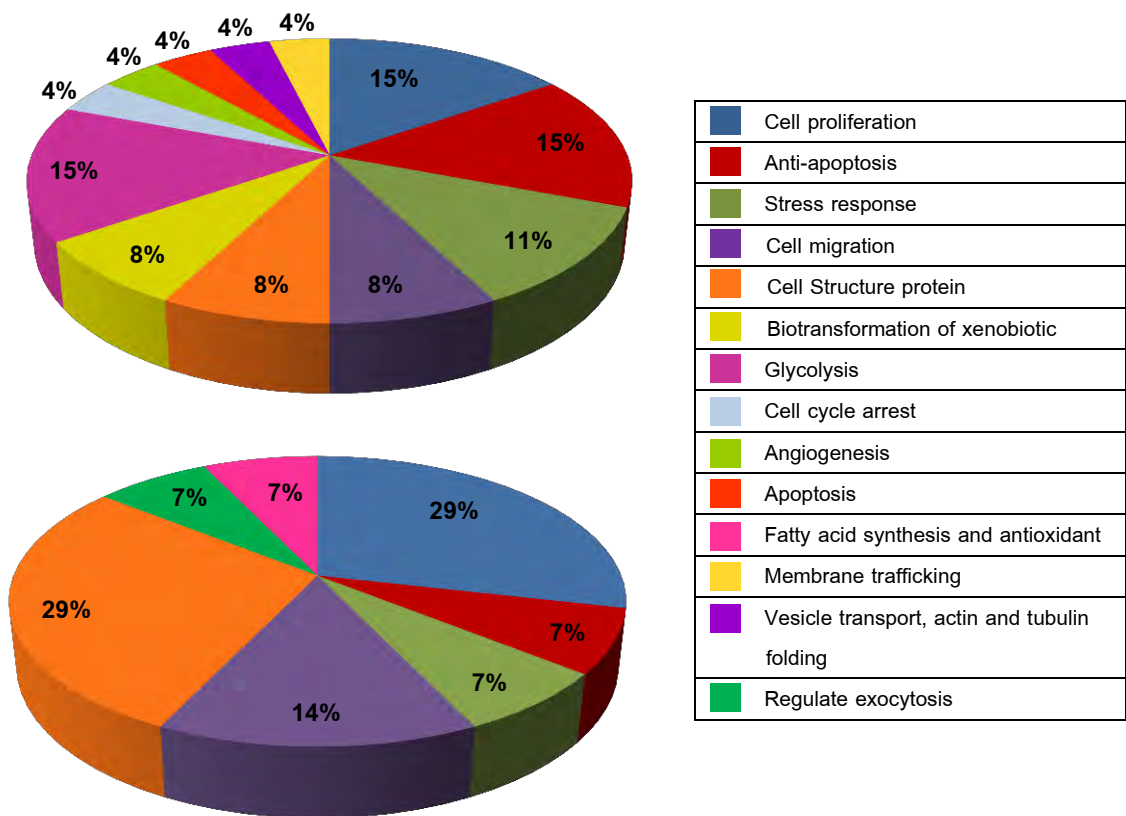


**Figure 4.3. Classification of identified proteins from LC/MS/MS based on function.** There are twelve groups classified for B-CPAP (top panel) and seven groups for FTC-133 (bottom panel), with five groups common to both cell lines as color coded.



















#### 4.6. Western blot analyses

Proteins were separated by using 12.5% SDS-PAGE and then proteins were electrotransferred onto PVDF membrane. After blocking membrane with 5% bovine serum albumin (BSA), proteins on membrane were probed with antibody against annexin A1 (1:1000, Chemicon International Inc.), annexin A2 (1:1000, Abcam Inc.), heterogeneous nuclear ribonucleoprotein K or hnRNP K (1:500, Cell signaling Technology Inc.), 14-3-3 Sigma (1:500, Abcam Inc.), pyruvate kinase M2 or PKM2 (1:1000, Santa Cruz Biotech Inc.), enolase (1:1000, Abcam Inc.), glyceraldehyde-3-phosphate dehydrogenase or GAPDH (1:1000, Abcam Inc.), triosephosphate isomerase or TPI (1:2000, Abcam Inc.) and tubulin as loading control (1:5000, Cell signaling Technology Inc.). Then membranes were incubated with secondary antibody and washed by TBS/T. The membranes were incubated with enhanced chemiluminescent reagent for 5 minutes and then exposed to film. Films were scanned by using Labscan 5.0 and intensities of bands were measured by ImageQuant TL program.

Figure 4.4 shows the one-dimensional Western blot results of eight antibodies as compared to tubulin as loading control. Intensities of each band were quantified and compared to the percent volumes from two-dimensional gel electrophoresis, as shown in Figure 4.5. Three proteins, glyceraldehyde-3-phosphate dehydrogenase, annexin A2 and pyruvate kinase M2, did not show corresponding changes of intensities from the 1D immunoblots. This does not mean that the expression of these proteins were not altered, as 1D immunoblots show total proteins that can be detected by the primary antibodies but would miss specific isoforms that can be detected in 2DE. Two-dimensional immunoblots would be necessary to confirm the differential expression of different isoforms of the same protein.

Annexins belong to a structurally related protein family that has calcium-, phospholipid- and membrane-binding motifs at carboxyl domain (23, 24). This family consists of 12 members including A1-A11 and A13 (23). Individual annexins have different molecular and cellular functions, e.g., vesicle trafficking, cell proliferation, cell differentiation, apoptosis, inflammation, blood coagulation and carcinogenesis (23, 24). The expression of individual annexins depends on the type of cancer. Annexin A1 is over-expressed in pancreatic adenocarcinoma and annexin A2 is overexpressed in metastasized breast cancer (23, 24). In contrast, loss of expression of annexin A1 was observed in breast adenocarcinoma (24).



Protein	Cell line	
	B-CPAP	FTC-133
Annexin A1		
Annexin A2		
hnRNP K		
PKM2		
GAPDH		
Enolase		
TPI		
14-3-3 Sigma		
Tubulin		

**Figure 4.4. One-dimensional Western blots of B-CPAP and FTC-133 cell lysates.** Eight primary antibodies were used for detection of proteins, as compared to tubulin as loading control.

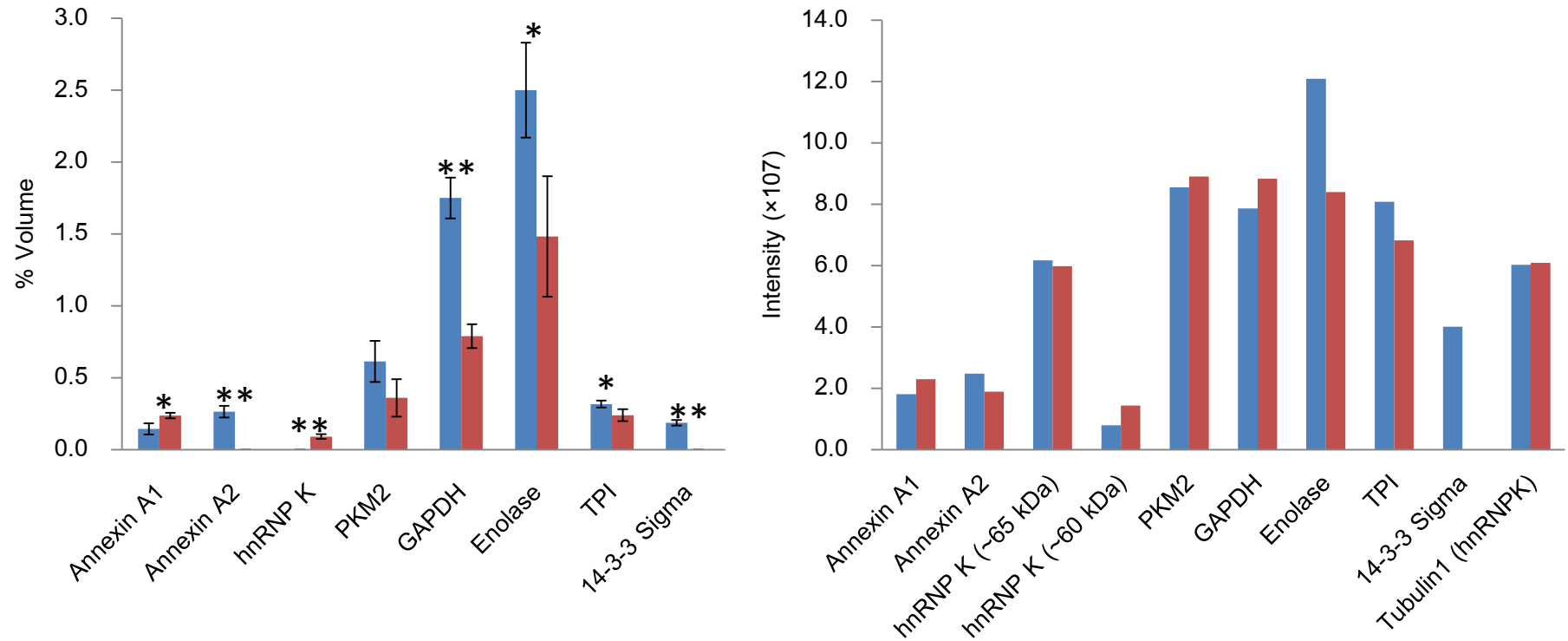


**Figure 4.5. Validation of eight proteins identified from LC/MS/MS.** The percent volumes from two-dimensional gel electrophoresis (left panel) were compared to the intensities of each band from one-dimensional Western blots. Blue and red bars represent B-CPAP and FTC-133 cell lines, respectively. p-values less than 0.05 were shown with \* and that less than 0.005 with \*\*.

Annexin A1 has been demonstrated to play a role in cancer progression, i.e., promote cell proliferation by acting as a substrate for epidermal growth factor receptor kinases and serine/threonine kinases. Moreover, over-expression of annexin A1 has been found to be related to increased anticancer drug resistance, which was postulated to result from the promotion of exocytosis of the drug (24). According from several studies, annexin A1 has the potential to be a biomarker of various types of cancer, which include lung cancer and hairy cell leukemia, as a negative biomarker for gastric cancer development and progression, and as a differentiation marker of thyroid cancer (24-26).

Over-expression of annexin A2 has been found in several types of cancer, including gastric carcinoma, breast cancer, colorectal cancer, pancreatic cancer, prostate cancer, high-grade gliomas and kidney cancer (23, 24). Annexin A2 exists in both monomeric and heterotetrameric forms. The monomeric form is located in the cytoplasm and the heterotetrameric form is located in the plasma membrane (23). Annexin A2 in the plasma membrane acts as a receptor or as a protease-binding protein, that binds to cathepsin B, plasminogen and tissue plasminogen activator. Moreover, it also acts as a binding protein for extracellular matrix proteins (23). Both functions of annexin A2 have importance for cancer cell invasion, migration and metastasis (23, 24).

Heterogeneous nuclear ribonucleoprotein K (hnRNP K) is a member of the hnRNP protein family. hnRNP-K is located in the nucleus, cytoplasm and mitochondria (27). It is found in several types of cancer, including prostate cancer, lung cancer, esophageal cancer, oral squamous cell carcinoma, colorectal cancer and nasopharyngeal carcinoma (27). hnRNP K has been suggested to play a role in cancer cell proliferation by promoting transcription and translation of human c-Src and c-myc genes (28).

Glycolysis is an essential metabolic pathway that supports energy (ATP) to organisms. All glycolytic enzymes are housekeeping proteins that are usually expressed in both normal and cancer cells (29). Especially for cancer cells, they require a lot of energy to support cell proliferation and overexpression of some glycolytic enzymes such as pyruvate kinase M2 (PK-M2), glyceraldehyde-3-phosphate dehydrogenase (GAPDH), enolase 1 (ENO1) and triose phosphate isomerase (TPI). These were found in various types of cancer

cell such as non-small cell lung cancer, intestinal tumor, etc. (30-34). The elevation of glycolysis also correlates with the increase of tumor aggressiveness and the worsening of cancer prognosis (31). Moreover, these glycolytic enzymes not only play role in energy production but each enzyme has other cellular effects too (29).

PK-M2 is a glycolytic enzyme that converts phosphoenolpyruvate (PEP) and ADP to pyruvate and ATP and this is also the rate limiting step in glycolysis (35). PK-M2 has two isoforms, which are tetrameric and dimeric forms. The tetrameric PK-M2 play a role in glycolysis that supports energy to cancer cells whereas the dimeric PK-M2 seemed to be an inactive form. However, this inactive pyruvate kinase also supports cancer cell growth by promoting the accumulation of nucleic acid, amino acid and phospholipid precursors, such as ribose-5-phosphate which is the precursor for nucleotide synthesis (36). Several evidences supported the correlation of dimeric PK-M2 to cancers in the gastrointestinal system including oesophageal, gastric, colonic and rectal cancer (30). Moreover, overexpression of the dimeric PK-M2 is also found in the plasma of breast, lung, renal and cervical cancers. The dimeric PK-M2 was detected in plasma and stool, which may suggest its role as a potential biomarker for several types of cancer, especially for gastrointestinal cancers (30, 36).

GAPDH is a glycolytic enzyme that phosphorylate glyceraldehyde-3-phosphophate to 1, 3-biphosphoglycerate by using  $\text{NAD}^+$  (29, 31). GAPDH has the ability to bind with DNA or RNA, which may participate in DNA repair and nuclear RNA export (29). Moreover, GAPDH also promotes cancer cell proliferation by acting as a component of Oct-2 coactivator OCA-S which involves S-phase-dependent histone -2B (H2B) transcription (29, 31). Recently, anti-apoptosis effect of GAPDH was investigated, i.e., GAPDH may protect cels from caspase-independent cell death (CICD). In contrast, GAPDH does not only support cancer cell progression but it can act as double-edged sword with negative effects to cancer cell too. GAPDH translocation to nucleus promotes cancer cell death through autophagy by up-regulation of autophagy protein ATG12 (31).

ENO1 or alpha enolase is a glycolytic enzyme that is present in all tissues. This enzyme dehydrates 2-phospho-D-glycerate (PGA) to phosphoenolpyruvate (PEP) and is

located in the nucleus, cytoplasm and cell surface (37). The function of ENO1 depends on its location. Cytoplasmic ENO1 is a catalytic enzyme in glycolysis, however nucleus and surface ENO1 have other cellular functions that both restrict and support tumor progression (29, 37). Genes of ENO1 may have alternative translation to yield 35-38 kDa *c-myc* promoter-binding protein-1 (MBP-1) (29). MBP-1 is located in the nucleus and suppresses *c-myc* gene expression through physically interacting with histone deacetylase. Suppression of *c-myc* proto-oncogene expression may decrease cancer cell proliferation and inhibit tumor progression (29, 37). In contrast, surface ENO1 does not restrain tumor progression but it encourages cancer metastasis by acting as a strong plasminogen-binding receptor involved in the degradation of extracellular matrix (ECM) components. Degradation of ECM may involve the spread of cancer cells in the body and promote tumor progression (37). Nowadays, ENO1 is a biomarker candidate for several types of cancer, i.e., autoantibodies of ENO1 has the potential to be a biomarker of non-small cell lung cancer (NSCLC) (32, 33).

TPI is a glycolytic enzyme that converts dihydroxyacetone phosphate to glyceraldehyde-3-phosphate (29). TPI not only plays a role in glycolysis but it may also be involved in anti-drug resistance of cancer, such as human gastric cancer cells (38). Nowadays, several studies support that TPI and its autoantibodies have the potential to be biomarkers of various cancers, including lung squamous cell carcinoma and breast cancer (34, 39).

14-3-3 $\sigma$  is a member of seven highly homologous protein 14-3-3 family, which include  $\alpha/\beta$ ,  $\gamma$ ,  $\epsilon$ ,  $\zeta$ ,  $\eta$ ,  $\sigma$ , and  $\theta/\tau$  (40). These proteins are present in several human tissues and have various cellular functions depending on their ligands (40). 14-3-3 $\sigma$  has been shown to have importance in cell cycle regulation, cell proliferation and apoptosis (41). Reduction or loss of 14-3-3 $\sigma$  expression was found in various types of cancer including breast, liver, prostate, head and neck and endometrium through hypermethylation of 14-3-3 $\sigma$  gene (41). Cancer cells tend to inhibit expression of 14-3-3 $\sigma$  because this protein regulates cell cycle arrest by binding to phosphorylated cdc2 and prevent cdc2-cyclin d-B1 complex that cause G2/M phase arrest, thereby acting a tumor suppressor protein (40, 41). However, this protein also promotes cancer cell survival by binding and inhibiting pro-apoptotic factor. 14-3-3 $\sigma$  could bind to Bax and/or Bad which are pro-apoptotic factors and prevent translocation of

these factors from the cytoplasm to mitochondria and also inhibit mitochondria-dependent apoptosis or cell death. This anti-apoptotic property of 14-3-3 $\sigma$  may correlate with poor response to treatment in breast, colon, lung and pancreatic cancers (41).

#### **4.7. Conclusion**

One hundred and one spots were detected to be differentially expressed in papillary and follicular cell lines. Forty spots were identified and eight proteins were validated using one-dimensional Western blots. Five proteins, which include annexin A1, heterogeneous nuclear ribonucleoprotein K, 14-3-3 Sigma, enolase and triosephosphate isomerase, exhibited altered protein expression with the most significant being 14-3-3 Sigma, enolase and hnRNP K. These five proteins may be used as a panel for the differential diagnosis of papillary carcinoma from follicular carcinoma.

## Chapter 5. Concluding remarks

Early on, we have anticipated problems with this project. The limiting factor of the proposed research is human specimens from our collaborator. This is the reason why we had to backtrack from studying cathepsin B from human tissues to studying in thyroid cancer cell lines. Unfortunately, the expression of cathepsin B from any of the studies cell lines was very low, almost only detectable with the high sensitivity of immunoblotting technique. This led us to request a one-year extension to rethink our project and propose to use proteomic technology to identify potential biomarkers for distinguishing well-differentiated thyroid cancers.

The activity of cathepsin B was indeed greater in papillary carcinoma than follicular adenoma tissues by eleven-fold. This activity is specific for cathepsin B as the ability to cleave substrate was completely abolished in the presence of inhibitor, CA-074. Three isoforms were detected in follicular adenoma and papillary carcinoma tissues with differential expression. Post-translational isoforms of cathepsin B were detected using specific gel stains for phosphorylation and O-linked N-acetylglucosamine glycosylation (O-GlcNAcylation).

When comparing the presence of cathepsin B in papillary carcinoma (B-CPAP), follicular carcinoma (FTC-133) and anaplastic carcinoma (8305C) cell lines, it was difficult to discern which spot corresponded to cathepsin B using Coomassie Blue staining for two-dimensional SDS-PAGE. The intensities in the 2-D SDS-PAGE of all forms of cathepsin B were faint, thereby requiring the increased sensitivities gained by immunoblotting. Two-dimensional immunoblots using two primary antibodies from different vendors revealed differential expression of active and heavy chain of cathepsin B isoforms in B-CPAP and FTC-133 cells. However, different isoforms of active cathepsin B in anaplastic (8305C) cell line were observed using one monoclonal antibody against cathepsin B from Calbiochem and not from R&D Systems. Different anti-cathepsin B antibodies could have different epitopes that bind to different parts of cathepsin B, thus selective to the monoclonal antibody from CalbioChem.

This led us to conclude that we would not be able to get enough cathepsin B from both tissues and cell lines for purification and characterization as proposed. We therefore decided to study FTC-133 and B-CPAP cell lines to obtain global protein patterns and distinguish differential protein expression for biomarkers for diagnosis. One hundred and one spots were detected to be differentially expressed in the two cell lines. Forty spots were identified using LC/MS/MS and eight proteins were validated using one-dimensional Western blots. Annexin A1,

heterogeneous nuclear ribonucleoprotein K, 14-3-3 Sigma, enolase and triosephosphate isomerase, exhibited altered protein expression with the most significant being 14-3-3 Sigma, enolase and hnRNP K, all of which corresponded to the differential protein expression from 2D SDS-PAGE. These five proteins may be used as a panel for the differential diagnosis of papillary carcinoma from follicular carcinoma, which would require further validation on human thyroid cancer tissues.



## Chapter 6. References

1. National Cancer Institute [homepage on the Internet]. Bethesda, Maryland [cited 2009 July 6] Available from: <http://www.cancer.gov/cancertopics/pdq/treatment/thyroid/HealthProfessional/page2>
2. SEER Fact Stat Sheet [homepage on the Internet]. Bethesda, Maryland [cited 2009 July 6] Available from: <http://seer.cancer.gov/statfacts/html/thyro.html>
3. Attasara P, editor. Cancer Registry 2006. [Online]. 2007 Available from: <http://www.nci.go.th>)
4. Thyroid.org [homepage on the Internet]. 2008 Falls Church, Virginia [cited 2009 July 15] Available from [http://www.thyroid.org/patients/patient\\_brochures/cancer\\_of\\_thyroid.html](http://www.thyroid.org/patients/patient_brochures/cancer_of_thyroid.html)
5. Srisomsap C *et al.* J. Proteomics 2002;2:706-12
6. Choudhury SD *et al.* Molecular and Cellular Biochemistry 1997;177:89-95
7. Atlas of Genetics and Cytogenetics in Oncology and Haematology [homepage on the Internet] 2009 Poitiers, France [cited 2009 July 15] Available from [http://atlasgeneticsoncology.org/Genes/CTSBID\\_40202ch8p23.html](http://atlasgeneticsoncology.org/Genes/CTSBID_40202ch8p23.html)
8. MacGregor RR *et al.* Journal of Biological Chemistry 1979;254:4423-7
9. Nomura T and Katunuma N. Journal of Medical Investigation 2005;52:1-9
10. Turk D *et al.* V. FEBS Letters 1996;384:211-4
11. Musil D *et al.* EMBO Journal 1991;10:2321-30
12. Nagler D *et al.* Biochemistry 1997;36:12608-15
13. Takahashi K *et al.* Journal of Biochemistry 1979;85:1053-60
14. Takahashi T *et al.* Journal of Biological Chemistry 1986;261:9368-74
15. Deval C *et al.* Biochemistry and Cell Biology 1990;68:822-6
16. Mach L *et al.* Biochemical Journal 1992;282:577-82
17. Docherty K and Philips ID. Biochimica et Biophysica Acta 1988;964:168-74
18. Moin K *et al.* Biochemical Journal 1992;285:427-34
19. Sawangareetrakul P *et al.* Cancer Genomics and Proteomics 2008;5:117-22
20. Deechongkit S *et al.* Journal of Pharmaceutical Sciences 2006;95:1931-43
21. Lirdprapamongkol K *et al.* Journal of Ethnopharmacology 2003;86:253-256
22. Salajegheh A *et al.* Postgraduate Medical Journal 2008;84:78-82
23. Lokman NA *et al.* Cancer Microenvironment 2011;4:199-208
24. Mussunoor S and Murray G. Journal of Pathology 2008;216:131-40

25. Petrella A *et al.* Cancer Biology and Therapy 2006;5:643-7
26. Yu G *et al.* Clinical and Experimental Metastasis 2008;25:695-702
27. Barboro P *et al.* British Journal of Cancer 2009;100:1608-16
28. Carpenter B *et al.* Biochimica et Biophysica Acta (BBA)-Reviews on Cancer 2006;1765:85-100
29. Kim JQ and Dang CV. Trends in Biochemical Sciences 2005;30:142-50
30. Hardt P *et al.* British Journal of Cancer 2004;91:980-4
31. Colell A *et al.* Cell Death and Differentiation 2009;16:1573-81
32. He P *et al.* Cancer Science 2007;98:1234-40
33. Chang YS *et al.* Clinical Cancer Research 2003;9:3641-4
34. Zhang XZ *et al.* Cancer Science 2009;100:2396-401
35. Lyssiotis CA *et al.* Biomedical Research 2012;23:213-7
36. Mazurek S *et al.* Seminars in Cancer Biology 2005;15:300-8
37. Liu KJ and Shih NY. Journal of Cancer Molecules 2007;3:45-8
38. Wang X *et al.* Journal of Cancer Research and Clinical Oncology 2008;134:995-1003
39. Tamesa MS *et al.* Electrophoresis 2009;30:2168-81
40. Hermeking H and Benzinger A. Seminars in Cancer Biology 2006;16:183-92
41. Li Z *et al.* American Journal of Translational Research 2009;1:326